

Rothamsted Repository Download

A - Papers appearing in refereed journals

Mohammed-Beigi, H., Aliakbari, F., Sahin, C., Lomax, C., Tawfike, A., Shafer, N.P., Amiri-Nowdijeh, A., Eskandari, E., Moller, I.M., Hosseini-Mazinani, M., Christiansen, G., Ward, J. L., Morshedi, D. and Otzen, D.E
2019. Oleuropein derivatives from olive fruit extracts reduce α -synuclein fibrillation and oligomer toxicity. *Journal of Biological Chemistry*. 294, pp. 4215-4232.

The publisher's version can be accessed at:

- <https://dx.doi.org/10.1074/jbc.RA118.005723>

The output can be accessed at: <https://repository.rothamsted.ac.uk/item/8w908>.

© 17 January 2019, AUTHORS

Oleuropein derivatives from olive fruit extracts reduce α -synuclein fibrillation and oligomer toxicity

Hossein Mohammad-Beigi^{1*}, Farhang Aliakbari^{1,2}, Cagla Sahin^{1,3}, Charlotte Lomax⁴, Ahmed Tawfike⁴, Nicholas P. Schafer^{1#}, Alireza Amiri-Nowdijeh⁵, Hoda Eskandari¹, Ian Max Møller³, Mehdi Hosseini-Mazinani⁵, Gunna Christiansen⁶, Jane L. Ward⁴, Dina Morshedi^{2,*,} Daniel E. Otzen^{1,7,*}

From the¹ Interdisciplinary Nanoscience Centre (iNANO), Aarhus University, Gustav Wieds Vej 14, DK-8000 Aarhus C, Denmark² Department of Industrial and Environmental Biotechnology, National Institute of Genetic Engineering and Biotechnology, P.O. Box: 1417863171, Tehran, Iran³ Department of Molecular Biology and Genetics, Aarhus University, Forsøgsvej 1, DK-4200 Slagelse, Denmark⁴ Computational and Analytical Sciences Department, Rothamsted Research, West Common, Harpenden, Herts, AL5 2JQ, UK⁵ Department of Agricultural Biotechnology, National Institute of Genetic Engineering and Biotechnology, P.O. Box: 1417863171, Tehran, Iran⁶ Department of Biomedicine-Medical Microbiology and Immunology, Aarhus University, 8000 Aarhus C, Denmark⁷ Department of Molecular Biology and Genetics, Aarhus University, Gustav Wieds Vej 10C, DK-8000 Aarhus C, Denmark

Running title: Oleuropein derivatives reduce α SN fibrillation and toxicity

Present address: N.P. Schafer, Department of Chemistry, Center for Theoretical Biological Physics, Rice University, Houston, TX 77005, USA.

*Corresponding authors: (D.E.Otzen) Tel.: +45-20725238; dao@inano.au.dk; (D.Morshedi) morshedi@nigeb.ac.ir; (H. Mohammad-Beigi) beigi@inano.au.dk

Keywords: α -synuclein; amyloid; cell toxicity; Mediterranean diet; membrane permeabilization; neurodegeneration; oligomerization; olive polyphenols; Parkinson's disease; phenolics;

ABSTRACT

Aggregation of α -synuclein (α SN) is implicated in neuronal degeneration in Parkinson's disease and has prompted searches for natural compounds inhibiting α SN aggregation and reducing its tendency to form toxic oligomers. Oil from the olive tree (*Olea europaea* L.) represents the main source of fat in the Mediterranean diet and contains variable levels of phenolic compounds, many structurally related to the compound oleuropein. Here, using α SN aggregation, fibrillation, size-exclusion chromatography–multi-angle light scattering (SEC-MALS)-based assays, and toxicity assays, we systematically screened the fruit extracts of 15 different olive varieties to identify compounds that can inhibit α SN aggregation and oligomer toxicity and also have antioxidant activity. Polyphenol composition differed markedly among varieties. The variety with the most effective antioxidant and -aggregation activities, Koroneiki, combined strong inhibition of α SN fibril nucleation and elongation with strong

disaggregation activity on preformed fibrils and prevented the formation of toxic α SN oligomers. Fractionation of the Koroneiki extract identified oleuropein aglycone, hydroxy oleuropein aglycone, and oleuropein as key compounds responsible for the differences in inhibition across the extracts. These phenolic compounds inhibited α SN amyloidogenesis by directing α SN monomers into small α SN oligomers with lower toxicity, thereby suppressing the subsequent fibril growth phase. Our results highlight the molecular consequences of differences in the level of effective phenolic compounds in different olive varieties, insights that have implications for long-term human health.

Parkinson's Disease (PD), the second most common neurodegenerative disease, is characterized by the degeneration of dopaminergic neurons in the *substantia nigra pars compacta* due to deposition of intracellular inclusions known as Lewy Bodies (LBs). These deposits can spread from cell to cell in a prion-

like fashion (1–4), leading to rigid posture, uncertain pace, and resting tremor. The major component of LBs is the 140-residue protein α -synuclein (α SN) which consists of three main regions: an amphiphilic N-terminal part, a non-amyloid hydrophobic β -peptide component (NAC), and an acidic C-terminus. The NAC region makes up the fibril core of amyloid fibril (5). Although monomeric α SN is intrinsically disordered (5, 6), it readily aggregates to oligomers, protofilaments, and fibrils (7, 8). α SN aggregation is extremely complex and depends on many different pathways and factors (9). The most toxic species, oligomers accumulate in the early stages of the fibril formation process and are thought to cause membrane destabilization (10), cytoskeletal changes (11, 12), mitochondrial dysfunction (11, 13, 14), and enhanced oxidative stress (11, 12, 15).

There has been an intense hunt for molecules which prevent α SN fibrillation and oligomerization and/ or reduce the toxicity of preformed aggregated species. Inhibiting the interaction of oligomers with membranes, decreasing the production of reactive oxygen species (ROS) (16) and / or curbing rising cytoplasmic Ca^{2+} levels are very challenging.

The olive tree (*Olea europaea*) is major source of fat in the Mediterranean diet (MeDi) (17), characterized by high plant food content. The MeDi is rich in antioxidants found in olive or other plant foods which may help lower oxidative stress in brain aging by affecting the expression of genes related to oxidative stress and markers of lipid oxidation (18) as well as protecting cells against oxidative damage (19). Olive phenolic compounds protect against a number of chronic degenerative conditions and are also implicated in the antioxidant, analgesic, anti-inflammatory, antitumor, antiviral properties of the olive (20, 21). They also inhibit self-assembly of A β 42, tau and α SN (22–24) into amyloids and toxic aggregates, possibly by preventing π - π and /or hydrophobic interactions (25, 26) and by redirecting these proteins into alternative nontoxic aggregates. Palazzi et al showed that oleuropein aglycone keeps α SN unfolded, rescues cells from oligomer toxicity, probes disaggregation of α SN aggregation, and prevents α SN binding to membranes (27). It has also been shown that olive biophenols could reduce the

enzyme-induced toxicity associated with the oxidative stress involved in the progression of Alzheimer's disease (AD) (28). Among these compounds, some such as phenolic acids and flavonoids are found in many fruits. However, the secoiriods are present exclusively in plants belonging to the family of Oleaceae which includes *Olea europaea* L. (29). Secoiriods include oleuropein (responsible for the bitter taste of olive fruits) and structurally related glucosides. The content of the polyphenols of olive fruit depends on the olive cultivar and the fruit ripening stage (30, 31). There are hundreds of olive varieties, classified based on their origin. Selection and promotion of beneficial polyphenol- rich olive varieties for long-term use may help combat PD at the population level.

While we do not claim that overall effects of a Mediterranean diet can be reproduced in their entirety by one or a few specific compounds, it is of basic interest to compare different olive varieties and establish causal relationships explaining their different effects. Comparison of complex mixtures such as different olive varieties under the controlled conditions has the potential to provide simple and straightforward information about the most important contributors to anti-aggregative and thus potentially anti-PD effects. Accordingly, we systematically screened extracts from different olive varieties for their ability to inhibit α SN fibrillation and formation of toxic aggregates. The assays monitored (a) kinetics, extent and end products of α SN fibrillation; (b) formation of toxic oligomers, disaggregation of preformed fibrils, induced changes in α SN through interaction with anionic vesicles and vesicle permeabilization induced by oligomers in the presence and absence of the extracts, and (c) toxicity of both extracts and α SN aggregates formed in the presence of extracts. The assays identified the extract, that most efficiently inhibited α SN fibrillation. The best extract in inhibiting α SN fibrillation was fractionated and the compounds present in these fractions were identified by LC-MS analysis.

Results

Selection of Olive Fruits and Preparation of the Extracts

Methanolic extracts were obtained from fruits of different olive varieties (Table S1). Of these, the Mediterranean varieties Koroneiki, Arbequina, and Picual are the world's most prestigious varieties for super high density cultivation systems with excellent oil quality characteristics. (32). Zard, Mari, and Rowghani are three prevailing varieties in Iran primarily used in olive oil production. The third group consisted of nine Iranian Tarom olive varieties (T10, T15, T16, T17, T18, T20, T22, T23 and T24).

Screening against α SN Aggregation Based on ThT Screening Assays

We first screened extracts for their ability to inhibit α SN aggregation using different ThT-based plate reader assays. α SN aggregation in PBS buffer was accelerated by shaking in the presence of glass beads (31).

In the fibrillation assay, all 15 extracts showed an aggregation-inhibitory effect at 0.025 and 0.3 mg/mL by reducing the end-point ThT fluorescence level, though to different extents. At 0.3 mg/mL, 7 of the 15 extracts (T10, T17, T20, T23, T24, Rowghani, and Koroneiki, in blue in Supplementary Fig. S1A and B) reduced end-point ThT levels to 1-15 % of the control in the absence of extracts. The following experiments described in this paper focus only on these most effective 7 extracts. Dose-response curves were then recorded (Fig. 1A) and the normalized maximum ThT intensity (Fig. 1B) was used to obtain IC_{50} values (Eq.1) of the 7 top-ranked extracts (Fig. 1C). Here, the Koroneiki extract emerged as the best inhibitor. The Finke-Watzky model (Eq. 2) was fitted to the ThT kinetic data (kinetic data are summarized in Fig. 1D-F) to obtain two central parameters, namely $t_{1/2}$ (the time required to produce half the total product) and ν (the rate of growth at $t_{1/2}$), from which the lag or nucleation time t_N could be calculated. The extracts reduced the level of fibrillation to different extents. All extracts except T24 produced a concentration-dependent reduction of ν and increase of $t_{1/2}$ compared to control.

Far-UV circular dichroism spectroscopy (CD), SDS-PAGE, and TEM images validated ThT data by providing independent measurements of the extent of fibrillation and the structure of the final aggregates. Remarkably,

several of the extracts maintained α SN in a largely unfolded conformation (Fig. 2A-C), particularly at 0.3 mg/mL extract. The normalized β -sheet content (%) of α SN is shown in Fig. 2D. The Koroneiki extract was particularly effective at retaining the unfolded conformation of α SN, and its preeminence compared to the other extracts became more obvious as the extract concentration was reduced to 0.15 and 0.1 mg/mL. T17, T20, T23, and T24 were least efficient in this regard, in good agreement with the ranking from the fibrillation assay.

SDS-PAGE was used to analyze the amount of soluble α SN in the supernatant after centrifugation. The 7 extracts significantly increased the amount of monomer left in the solution after 24 h incubation (Fig. 2E and Fig. S2). Low, but detectable amounts of dimers and larger aggregates are also visible in the presence of some of the extracts. For additional confirmation, the supernatants of the incubated samples of α SN in the absence and presence of 0.3 mg/ml of Koroneiki were run on a gel filtration column. As shown in Fig. 2F, Koroneiki significantly increased the amount of monomer left in the solution after 24 h incubation. Two populations of oligomers were also detectable after gel filtration of samples with Koroneiki.

The effect of 0.3 mg/ml extract on the morphology of endpoint α SN aggregates was analyzed by TEM (Fig. 2G and associated table). While the limited quantitative output from these TEM analyses preclude detailed comparison with ThT parameters such as lag time and growth rates, there is good qualitative agreement: Koroneiki and Rowghani extract completely suppress fibril formation and only oligomers are detectable, just as they very efficiently suppress ThT signals. The other extracts reduce fibril formation to a somewhat smaller extent, but still lead to significant reductions compared to the control, consistent with their overall reduction of ThT signal.

Olive Fruit Extracts Induce Formation of Different Oligomers

To study the effect of the extracts on the formation of soluble aggregates, we prepared oligomeric species of α SN in the presence and

absence of 0.15 mg/ml extracts. While fibrillation of α SN is a slow process with lag times of 10-20 h depending on protein concentration (33), oligomer formation occurs over a few (<5) hours. We have previously shown that during the oligomerization (900 rpm, 37 °C), α SN forms two populations of oligomers, largely elongated oligomers and small spherical oligomers, which increase slowly over time (7, 34). The small oligomers, estimated to contain ~ 30 monomers, form a compact prolate ellipsoid core with a number of flexible chains protruding from the surface into the solution, while the larger oligomers are concatemers of the smaller ones (34).

We used SEC-MALS (Fig. 3A for Koroneiki and Fig. S3 for the others), a technique in which species are separated according to hydrodynamic radius on a SEC column, after which the concentration of the species are obtained from the peak area under the MALS peaks. We did not estimate oligomer concentration based on absorption at 280 or 215 nm since extract binding to the oligomers could affect absorption. Instead we used MALS data to allow more direct comparison of oligomer yields. This ranked the amount of large oligomers formed in the presence of the extracts in the following order: T23 > Rowghani > T10 \approx T17 \approx T24 > Koroneiki > T20, which differed significantly from that of the small oligomers (Koroneiki > T10 > T23 \approx Rowghani \approx T10 \approx T17 \approx T 24). In all cases, the level of monomers was relatively unchanged, indicating that most α SN remained unaggregated.

Olive Fruit Extracts Disaggregate Preformed Fibrils

We next used gel filtration to address whether overnight incubation with extracts could disaggregate existing α SN fibrils. We monitored this process by absorption at 215 nm, since we were mainly concerned with the appearance of soluble α SN. Addition of olive extracts led to an increase in the monomer peak, as well as the formation of soluble oligomers (eluting at 5-10 ml), particularly in the presence of 0.15 mg/mL of Koroneiki extract (Fig. 3B). Additional peaks eluting after the α SN monomer peak are C-terminal fragments of α SN formed by chemical cleavage after long-term incubation (C. Sahin et al., unpublished results). Thus existing fibrils

could be disaggregated by Koroneiki extract at concentrations which also completely inhibited aggregation. The other extracts had less dramatic effects (Fig. S4), though T17 and T20 extracts in particular increased the monomer population to some extent.

Olive Fruit Extracts Inhibit Fibril Elongation

To determine whether or not the extracts could affect elongation of existing fibrils, short fibrillar seeds (5%) were added to monomeric α SN. This bypasses the nucleation step and allows us to study the elongation of existing fibrils. Koroneiki extract was the most effective inhibitor in both shaking and non-shaking assays, leading to a very extended lag phase of fibrillation (\approx 10 h) under shaking conditions and completely suppressing fibril growth over a 45 h observation period in the absence of shaking (Fig. 3C and D). The other extracts reduced elongation rates to different extents. T23 extract performed most poorly in both assays, while T17, T10, and T20 extracts performed quite well though not as well as Koroneiki extract. Thus, Koroneiki extract was the best inhibitor of both nucleation and fibril elongation.

Olive Fruit Extracts Do Not Inhibit the Change in α SN Structure Induced by Vesicles

Interaction with anionic phospholipid vesicles induces a major increase in α -helical structure in α SN (35) (Fig. 3E). Compounds such as squalamine can displace α SN from lipid membranes and decrease the α -helical content of α SN (36). However, even at the high concentration of 0.15 mg/ml, none of the extracts prevented monomeric α SN from forming an α -helical structure in the presence of anionic vesicles of DMPG (Fig. 3F). Consistent with this, the Koroneiki extract failed to show any effect at other concentrations (0.025-0.3 mg/ml, data not shown).

Olive Fruit Extracts Are Nontoxic, Show Antioxidant Activity, and Decrease the Level of ROS in OLN-93 Cells

We evaluated the antioxidant activity of the olive extracts at 0.02-0.12 mg/mL using the DPPH• assay. All extracts showed similar dose-response levels in this assay (Fig. S5A). Further, none of the extracts showed significant toxicity

on their own towards OLN-93 and SH-SY5Y cells according to the MTT assay (Fig. S5B and Fig. S5E).

We used DCFH-DA to evaluate extract effects on ROS production in OLN-93 cells. All extracts except T24 decreased free radical formation (Fig. S5C). Further, all extracts neutralized the deleterious effect of 100 μ M H₂O₂ (Fig. S5D) to the same concentration-independent extent.

Olive Fruit Extracts Induce Formation of Less Toxic Aggregates and Reduce the Cytotoxicity of Oligomers to the SH-SY5Y Cells

We evaluated the membrane permeabilization and cytotoxicity of aggregates formed during different stages of α SN fibrillation with and without extracts (Fig. 4A). Without extracts, the ability of aggregates to release calcein decreased as the aggregates aged over 24 h (Fig. 4B); several of the extracts, particularly Koroneiki, accelerated this decline. This suggests that aggregates formed in the presence of the extracts interact less with the membranes.

In the MTT cell viability assay with OLN-93 and SH-SY5Y cells, aggregates formed in the presence of the extracts showed less cytotoxicity than the extract-free α SN control samples (Fig. 4C and 4D). The aggregates were more toxic to OLN-93 cells (Fig. 4C) than to SH-SY5Y cells (Fig. 4D). While all extracts significantly enhanced viability of OLN-93 cells at the early stages (4, 8, and 12h), at 24 h this effect is just significant for T17, Rowghani, and Koroneiki extracts. However, for SH-SY5Y cells, this enhancement effect is retained for all extracts and all incubation times (Fig. 4D). A difference in response by different cell lines is not without precedent; we have also recently reported that SH-SY5Y and PC-12 cells (another neuronal cell line) differ in their sensitivity to α SN aggregates (37).

We needed to rule out that the reduced toxicity of aggregates formed in the presence of the extracts could be caused by a general effect of the extracts on the cells. Therefore, we treated SH-SY5Y cells with Koroneiki extract, incubated for 2 h, removed the solution and washed with PBS. Subsequently we added α SN aggregates both to extract-treated and untreated cells. We found no significant difference in aggregate

toxicity on the two cell types (data not shown), ruling out a general extract effect.

Mitochondrial disruption induced by the aggregates was evaluated by the release of lactate dehydrogenase (LDH) (Fig. 4E). The aggregates formed without the extracts increased LDH release by 60-72 % compared to control. However, LDH release was reduced significantly in cells treated with aggregates formed in the presence of the extracts. This is consistent with reduced cellular toxicity and confirmed that extracts reduce the toxicity of aggregates in the cell-based assays.

In the next step, the membrane permeabilization assay (Fig. 5A) was carried out to see if Koroneiki extract can decrease the membrane-disrupting ability of α SN oligomers, which permeabilize the membrane (and by inference induce toxicity in cells). Fig. 5B shows that Koroneiki extract only leads to an insignificant reduction in oligomer-induced permeabilization of anionic phospholipids in a calcein release assay. The Koroneiki extract itself does not lead to any calcein release and loss of vesicle integrity (data not shown).

We finally tested the Koroneiki extract for its effect on oligomer toxicity in a cellular context (Fig. 5C). Purified oligomers decreased viability by 28 % on their own but only by 15% in the presence of 0.15 mg/ml Koroneiki extract. Thus, Koroneiki extract not only led to formation of less toxic and less cell-permeabilizing oligomers (Fig. 4 B-D), but also protected SH-SY5Y cells against preformed toxic oligomers (Fig. 5C). Koroneiki extract at 0.015 mg/ml did not significantly reduce the toxicity of oligomers (data not shown).

The Chemical Composition of Different Extracts

HPLC analysis of the most effective extracts revealed the same qualitative but different quantitative phenolic composition for major components (Fig. S6). For more detailed studies, the Koroneiki extract was fractionated by UHPLC (Fig. S7), after which the inhibitory effect of the fractions was studied and the best fractions in inhibiting α SN fibrillation and reducing toxicity of α SN oligomers were analyzed on LC-MS to identify the compounds involved.

Identification of the Most Effective Fractions

In the first step, the effect of fractions of the Koroneiki extract on α SN fibrillation was studied at two different concentrations. These are designated L and H (Low and High). L and H fractions are obtained from 1 mg/ml and 3 mg/ml Koroneiki extract, respectively, which implies that the concentration of the fractions in the fibrillation assays are much less than 1 mg/ml and 3 mg/ml. The most effective fractions (5, 6 and 17-26) are indicated in red in Fig. S8A and S8B, while the time profiles of fibrillation are shown in Fig. S9. CD and TEM images were used to confirm the ThT data and better understand their effect on α SN fibrillation. CD data (Fig. 6A and 6B) show that the most effective fractions maintained the unfolded secondary structure of α SN. The effect of the fractions at 3 mg/mL on the morphology of endpoint α SN aggregates was analyzed by TEM (Fig. S10). In the presence of the fractions, either only oligomers (f5, 18, 21, 23, and 25) or both short fibrils and oligomers (f6, 17, 19, 20, 24, and 26) were detectable. In contrast, the control sample without the Koroneiki extract fractions only showed long straight fibrils.

To determine whether or not the fractions affect elongation of existing fibrils, we incubated monomeric α SN with 5% α SN seeds. Fractions 19, 20, 21, 22, and 23 were the best inhibitors of secondary nucleation (Fig. 6C). The other fractions did not completely inhibit seeded fibrillation but instead decreased the rate of elongation, increasing the time it took for the ThT fluorescence to reach a plateau level.

The effect of the top 12 fractions identified in the ThT assay on the level of small and large oligomers and their ability to disaggregate existing fibrils of α SN was also studied. Fractions 6, 18, 21, 22, 23 led to the formation of more small oligomers (Fig. S11A). Disaggregation of α SN fibrils by Koroneiki fractions also led to the formation of soluble oligomers (Fig. S11B) and fractions 5, 20, 24, 25, 26 were the most effective.

Identification of the Antioxidant Activity and Toxicity of Different Koroneiki Extract Fractions

We evaluated the antioxidant activity of the Koroneiki fractions using the DPPH• assay. Fractions with the most inhibitory effect (f5, 6, 17-26) showed more inhibition (%) and

scavenging ability (Fig. S12A). When these fractions were incubated with OLN-93 and SH-SY5Y cells, they showed no significant toxicity at 1 and 2 mg/mL (Fig. S12B and S12C); however, fractions 19, 21, 23, and 25 were slightly toxic to OLN-93 cells at the highest concentration tested (3 mg/mL).

The Most Effective Fractions Induce the Formation of Less Toxic Aggregates

The same toxicity assay as for whole extracts was used to evaluate the toxicity of formed aggregates during the fibrillation process either in the presence or absence of the Koroneiki fractions. The calcein release assay showed a reduction in the interaction of the aggregates formed up to 24 h in the presence of fractions with the membranes compared to the control samples (Fig. 6D). In the cell assay on both OLN-93 and SH-SY5Y cells, the toxicity of control aggregates formed up to 8 h increased and then decreased slightly. Aggregates formed in the presence of the Koroneiki fractions also generally showed an increase in cytotoxicity at early stages, but the levels of toxicity were reduced compared to control, in particular for fraction 25 (Fig. 6E and F). Overall, the LDH assay in SH-SY5Y cells also confirmed these data (Fig. 6G).

Separation and Identification of Phenolic Compounds in the Most Effective Fractions

We used LC-MS analysis of the most effective Koroneiki fractions to separate and identify major components of these fractions. Identification of the compounds was done based on accurate mass measurements of the $[M-H]^-$ ion and their MS/MS fragmentation patterns as documented in the literature. The total ion current (TIC) profiles of representative olive fractions are presented in Fig. S13. Data obtained from high resolution MS analysis of the fractions are summarized in Table S2. The major compounds in each fraction are listed in Table S3 and indicated on the TIC profiles of individual fractions (Fig. S13). It is clear that the single largest family of compounds consists of oleuropein and derivatives thereof. For additional insight, we tested individual compounds identified in the Koroneiki fractions, namely verbascoside, loganin, rutin, elenolic acid, 3-Hydroxytyrosol, and oleuropein. The compounds

effects on α SN fibrillation were tested through ThT-based kinetics, CD spectroscopy and TEM imaging (Fig. 7). ThT data (Fig. 7A) show that verbascoside, elenolic acid, 3-hydroxytyrosol and oleuropein completely inhibit fibrillation at 50 (verbascoside) or 100 μ M (all other compounds), comparable to the effect of EGCG (38). The CD data (Fig. 7B) also show that these compounds keep α SN in its monomeric unfolded state better than other compounds. Finally, TEM images of α SN after incubation in the presence of oleuropein confirm the absence of fibrils (Fig. 7C).

Correlating the Change in the Chemical Compositions of Extracts with their Inhibitory Effect

We also analyzed extracts from developing fruits to correlate the change in the chemical composition of the extracts with their inhibitory effect. During the ripening process and fruit development, the phenolic content changes (31). Accordingly, we collected olive fruits at different ripening time and the effect of the extracts was tested on α SN fibrillation. The HPLC data and the effect of the extracts are shown at Fig. S14. Then the average values of the end ThT values of α SN aggregation in the presence of different amounts of olive extracts (the 9 top-ranked extracts as well as extracts of fruits collected at different ripening times) were combined with the HPLC data of the olive samples to analyze the effect of different compounds in the extracts. The “peakutils” Python package was used to identify peaks in the HPLC data. Finally, a correlation analysis was performed to determine which peaks have correlated amounts across all of the samples. This analysis confirmed that the compound eluting as oleuropein aglycone, which also shows the highest *m*-value as a measure of its anti-fibrillation potency, is of interest since the level of that compound was not well correlated with other compounds and was therefore more likely to be responsible for the difference in inhibition across the extracts (Table 1). Comparison of HPLC chromatograms of extracts of fruits picked at different ripening time with their inhibitory effect (Fig. S14) revealed that the extracts with higher level of oleuropein aglycone had more inhibitory potency; in contrast, the levels of other

compounds were lower compared to the less effective extracts.

Discussion

In PD, α SN aggregation initiates a cascade of molecular events leading to neuronal death. As a consequence, the identification of small molecules able to interfere *in vivo* with aggregation of α SN is a vital strategy against PD. Here we address three questions to identify olive oils with maximal anti-aggregative effects:

- 1) What is the mechanism behind the inhibiting effect of beneficial polyphenols?
- 2) Can these polyphenols lead to the formation of less toxic aggregates?
- 3) How do the level of beneficial polyphenols change with time?

The Best Extracts in inhibiting α SN fibrillation Inhibit Both Nucleation and Elongation of α SN

A summary of the efficacy of the olive extracts and the Koroneiki extract fractions in different assays is shown in Tables 2 and 3, respectively. We scored each assay between 0 and 1 and then determined the final ranking. We classified extracts of 7 out of 15 different olive varieties according to their efficacy in inhibiting distinct steps of α SN aggregation (nucleation and elongation). Although the ranking differed slightly in different assays, all assays emphasized the remarkable inhibitory effect of the Koroneiki extract as the best inhibitor of both nucleation and elongation. Koroneiki, 'the queen of olives', is a variety with particularly good oil quality characteristics, making it the main olive oil produced in Greece (39). Koroneiki and T20 varieties were most effective in the disaggregation assay, whereas Rowghani, which had performed well in the other assays, performed poorly here. These extracts may interact with the hydrophobic residues of β -sheet and cause disaggregation of amyloid fibrils. The different rankings indicate that these extracts are likely to bind both nuclei and fibril surfaces and ends, but to different extents.

The Best Extracts in inhibiting α SN fibrillation Favor Less Toxic Oligomeric Species

Inhibition of aggregation could bypass the formation of toxic prefibrillar aggregates and direct α SN towards less toxic aggregates. SEC analysis and SDS-PAGE were used to analyze the aggregates that form in the presence of the extracts. Interestingly, Koroneiki extract, which was the best inhibitor, also ranked top in the formation of small oligomers and only led to a low production of large oligomers, while the T23 extract, which performed poorly in all other assays, strongly favored large oligomers. The SDS-PAGE results also indicate that the great majority of the α SN remains monomeric and the TEM images showed a reduction in longer fibrils at the fibrillation assay endpoint in the presence of the extracts. We therefore conclude that the most promising extracts inhibit α SN amyloidogenesis by retaining α SN in the monomeric state, and incorporating minor amounts of α SN monomers into highly stable oligomers that are non-cytotoxic and off-pathway to fibrillogenesis (16), thereby inhibiting the subsequent growth phase (Fig. 8).

This change in the aggregation process also reduces cytotoxicity. Co-incubation of monomeric α SN with Koroneiki extracts lead to the formation of aggregates that – particularly after longer incubation – permeabilized membranes significantly less than the control aggregates and were less toxic to OLN-93 and particularly to SH-SY5Y cells. Some compounds are known to inhibit the membrane interactions of preformed α SN oligomers (16, 40). This is not the case for Koroneiki extract, which did not reduce the interaction of α SN monomers or preformed α SN oligomers with membranes, so the reduction in cytotoxicity of preformed α SN oligomers must derive from another as yet unknown mechanism, rather than by reducing membrane interactions.

α SN is susceptible to oxidative stress which in turn favors its aggregation (41), and oligomeric species formed in the aggregation process can induce oxidative stress (42). Therefore, extracts and compounds that inhibited both α SN aggregation and reactive oxygen species (ROS) production would be promising. The extracts themselves showed no toxicity to OLN-93 and SHSY5Y cells. All extracts showed significant antioxidant activity and neutralized the

deleterious effect of H_2O_2 on cells with different potency. This protective effect other than the scavenging of free radicals could be due to the effect at the molecular level of the cells such as activation of signaling cascades and regulation of calcium ion homeostasis (43).

Oleuropein aglycone, Hydroxyoleuropein aglycone, and Oleuropein Are Mainly Responsible for the Difference in Inhibition across the Extracts

An understanding of the molecular mechanism of olive extract-induced inhibition is complicated by the polyphenolic complexity as evidenced by LC-MS. In addition to polyphenols, such as flavonoids found in many fruits, oleuropein and other glucosides structurally related to this compounds are present exclusively in olive plants. Using the same assays as used for ranking the extracts, the inhibitory effect of fractions of the Koroneiki extract was tested on α SN fibrillation. Phenolic compounds present in the inhibitory extracts were identified as hydroxytyrosol, hydroxytyrosol glucoside, oleuside, rutine, verbascoside, 6'-(E)-p-coumaroyl-secologanoside, and compounds structurally related to oleuropein, such as dihydrooleuropein, hydroxyoleuropein, oleuropein glucoside, hydroxyoleuropein aglycone, and oleuropein aglycone (Table S3). Some of these compounds are commercially available and the others can be chemically synthesized or isolated from olive sources. The effects of some of the compounds on fibrillation of proteins and their antioxidant potency have been studied before (22–24). The fractions containing the most effective compounds were ranked in different assays (Table S5). As shown for the extracts, the isolated fractions also have different effects in the assays used in this study (Table 3). Some extracts have more fibrillation inhibitory potency (f5, 19, 20, 21, 22, 24), some are better in inhibition elongation (f5, 6, 19, 20, 21, 22), some produce more small oligomers (f18, 21, 22), some are more effective in disaggregation of preformed fibrils (f5, 20, 24, 25, 26), and some of them were excellent in decreasing the formation of toxic aggregates (f5, 17, 20, 21, 26). Interestingly, all the fractions with the highest inhibitory effect (f5, 6, 17-26) showed higher ROS scavenging ability.

HPLC analysis showed that the content of the polyphenols of olive fruit depends on olive cultivar and ripening stage of the fruit, which leads to a different effect on the fibrillation process and the formed α SN species, antioxidant activity and ROS scavenging and toxicity. To correlate the change in the polyphenol content of the extracts with their inhibitory effect, we compared the level of the compounds based on the height of the peaks in each extract with the end ThT values in a correlation analysis (Table 1). This analysis shows that oleuropein aglycone, hydroxyoleuropein aglycone, and oleuropein are the main compounds responsible for the difference in inhibition across the extracts. Koroneiki as the most inhibitory cultivar contains the maximum level of oleuropein aglycone compared to the other varieties. This correlation in the extracts of same varieties picked at different ripening stages is also clear. Most of the compounds in olive oil result from spontaneous oleuropein hydrolysis and processing (44). The hydrolysis of oleuropein by an endogenous β -glucosidase during ripening leads to formation of oleuropein aglycone, which is the key compound responsible for the protective effect of olive oils. There are other studies on the inhibitory effect of oleuropein aglycone on fibrillation of aggregation-prone proteins. Palazzi et al (27) recently demonstrated that oleuropein aglycone hampers the growth of on-pathway α SN oligomers and favors growth of stable and harmless aggregates. Further, oleuropein aglycone reduces the toxicity of α SN aggregates by interfering with their binding to cell membrane components. These data are in accordance with our own findings that olive compounds rescue cells from the toxicity of α SN aggregates. Oleuropein aglycone also interferes with the *in vitro* aggregation of human amylin and A β 42 and redirects the aggregation pathway towards non-toxic aggregates, and interferes with A β 42 proteotoxicity *in vivo* in transgenic *C.elegans* strains expressing A β 42 by reducing plaque load and motor defect (20, 44, 45).

In summary, we conducted a systematic study of the effect of fruit extracts of different olive varieties on α SN fibrillation, oligomerization and toxicity, and antioxidant activity to select phenol-rich olive varieties with

maximal effective phenolic content to counteract the development of PD hallmarks. We conclude that the polyphenols in olive fruits play a significant role in protection against PD. More specifically, we conclude that polyphenols can reduce α SN aggregate toxicity through their antioxidant activity and direct aggregation towards non-toxic species. Our results contribute to the wider discussions concerning the mechanism of action of polyphenols in aggregation and toxicity prevention. Evaluation of the protection against PD by olive extracts and polyphenols in cell and animal models and development of nanocarriers to increase the bioavailability of olive polyphenols would be an interesting further step to drug development for PD. This will be useful not only for PD but also for assessing the potential of polyphenols in olive oils for future applications.

Experimental procedures

Materials

Penicillin–streptomycin, fetal bovine serum (FBS), and Dulbecco's Modified Eagle Medium (DMEM) were purchased from Gibco BRL (Gaithersburg, MD, USA). 1,2-dioleoyl-sn-3-phosphatidyl-glycerol (DOPG) were from Avanti Polar Lipids (Alabaster, AL). Lactate dehydrogenase (LDH) measurement kit was from Pishtazteb Co. (Iran). All other chemicals were from Sigma Aldrich (St. Louis, MO).

Olive Fruit Samples

Three distinct categories of olive varieties were studied (Table S1). The first group, the Tarom varieties (T), consists of nine Iranian olive varieties including T10, T15, T16, T17, T18, T20, T22, T23 and T24 (46). The second group consists of three Mediterranean varieties including Koroneiki, Arbequina and Picual. The third group consists of three major varieties in Iran including Zard, Mari, and Rowghani. All the studied olive trees were nearly 18 years old, reproduced by taking cuttings from the mother plant, irrigated and fertilized by a drip system at Tarom olive research station. All trees samples were in the same orchard under the same environmental conditions. Three replicated plants were studied. The fruits were picked at 180 days after full bloom (DAFB) corresponding to

different developmental stages for the different olive tree varieties. Samples were stored at -20°C on the same day of picking (47).

Extraction of Phenolic Compounds From Olive Fruits

The fresh mesocarp (3 g) was frozen in liquid nitrogen and ground to fine powder in a porcelain mortar. It was then mixed with methanol (12 mL) and vortexed for 1 min at 20°C. The resulting mixture was centrifuged (3500 rpm at 4°C) for 20 min. The supernatant was separated, lyophilized and stored at -20 °C.

Protein Production and Purification

Recombinant human α SN was expressed in *Escherichia coli* BL21(DE3) strain with a plasmid vector pET11-D using auto-induction (48). Briefly, the pelleted cells were resuspended in 100 mL osmotic shock buffer (30 mM Tris-HCl, 40 % sucrose, 2 mM EDTA, pH 7.2), and incubated for 10 min followed by centrifugation (9000 g, 20 °C, 30 min). The resulting pellet was resuspended in 90 mL ice-cold deionized water and 40 μ L of saturated $MgCl_2$ was added, followed by incubation on ice for 3 min. The supernatant after centrifugation (9000 g, 4 °C, and 20 min) was precipitated by titration with 1 M HCl to pH 3.5 and then incubated for 5 min. The supernatant was collected by centrifugation (9000 g, 4 °C, and 20 min) and immediately titrated to pH 7.5 with 1 M NaOH, filtered (0.2 μ m) and loaded on a Q-Sepharose column (HiTrap Q H P) pre-equilibrated with 20 mM Tris-HCl pH 7.5. Then, α SN was eluted with a NaCl gradient from 0.1-0.5 M. The fractions were analyzed using SDS-PAGE and the collected purified α SN was dialyzed exhaustively against deionized water, lyophilized and stored at -20 °C.

Protein and Extract Handling

Prior to use, freshly dissolved α SN in PBS buffer, pH 7.4, was filtered (0.2 μ m). Protein concentration was measured by absorbance measurements at 280 nm with a NanoDrop™ 1000 spectrophotometer (Thermo Scientific) using a theoretical extinction coefficient of 0.412 (mg/mL)⁻¹. All olive fruit extracts used in the screening assays were freshly dissolved in PBS buffer and filtered (0.2 μ m) prior to use.

Plate Reader Fibril Formation Assays

α SN fibril formation was carried out as described (33). Briefly, 150 μ L PBS solution containing 70 μ M (1 mg/ml) α SN, 40 μ M ThT and varying amounts of methanolic olive extracts was added to each well of a 96-well-plate (Nunc, Thermo Fischer Scientific, Roskilde, Denmark) with a 3 mm diameter glass bead, sealed with Crystal clear sealing tape (Hampton Research, Aliso Viejo, CA, USA). The fibrillation was followed at a Genios Pro fluorescence plate reader (Tecan, Mänerdorf, Switzerland) at 37 °C with 300 rpm orbital shaking between the readings for 12 min. Samples were excited at 448 nm and emission was measured at 485 nm.

The dose-response aggregation inhibition curves fitted a simple binding isotherm:

$$\frac{ThT_{end\ level}}{K_D + [Olive\ extract]} = (ThT_0 - ThT_{min})(1 - \frac{[Olive\ extract]}{K_D + [Olive\ extract]}) + ThT_{min} \quad (1)$$

where $ThT_{end\ level}$ is the ThT fluorescence level at the end of the fibrillation process at a given olive concentration, ThT_0 is the ThT fluorescence end level in the absence of compounds, ThT_{min} represents the ThT level at maximum inhibition, $[Olive\ extract]$ is the concentration of the olive extract and K_D is the mole ratio needed for half inhibition.

The Finke-Watzky (F-W) (49) equation was fitted to the normalized ThT fibrillation data:

$$F(t) = \frac{1}{1 + e^{-4v(t-t_{1/2})}} \quad (2)$$

$$t_N = t_{1/2} - \frac{1}{2v} \quad (3)$$

where $t_{1/2}$ is the time required to produce half the total product, v is the rate of growth at $t_{1/2}$ and t_N is the duration of the nucleation (lag) phase (31).

Seeding Experiments

The fibril elongation assays were performed using a plate reader setup with the same settings as for the fibrillation assay in the presence of 0.05 mg/mL seeds (corresponding to 3.5 μ M monomer) and 0.15 mg/ml olive extracts in a solution of 70 μ M monomeric α SN in 96-well plates. The snap-frozen mature fibrils were thawed and fragmented by sonication for 2 min on ice (pulse 5 s. on and 5 s. off) with an amplitude of 20 % on a QSonica Sonicators (Q500, Newtown, CT, USA) to obtain short fibrils, which were employed as seeds.

Fibril Disaggregation Assays

The fibril stock solution was prepared using the same setting as for the fibrillation assay and the fibrils. Aggregated α SN (35 μ M monomer equivalents) was incubated overnight either alone or with the olive extracts (0.15 mg/mL) at 37 °C. The solution was centrifuged (21000 g, 20 min) and the supernatant was injected onto a 24 mL Superose 6 10/300 gel filtration column (GE Healthcare Lifescience) at 0.5 mL/min to separate monomers and oligomeric species.

Preparation of Oligomers

α SN oligomers were prepared as previously described (16). Briefly, 12 mg/mL α SN was incubated in PBS buffer for 5 h at 37 °C and 900 rpm on an Eppendorf thermoshaker, TS-100, BioSan, Latvia. The sample was then centrifuged (21000 g, 10 min) to remove insoluble material and the supernatant was loaded on an a Superose 6 Prep Grade column, GE healthcare Life Sciences, Sweden, in PBS at 2.5 mL/min. Small oligomers were collected and were concentrated with 15 mL Amicon ultracentrifugal filters (Merck).

Preparation of Large Unilamellar Vesicles (LUVs)

LUVs were prepared as described (50). Briefly, 1, 2-dioleoyl-sn-3-phosphatidylglycerol (DOPG) or 1,2-dimyristoyl-sn-glycero-3-phospho-(1'-rac-glycerol) (sodium salt) (DMPG) was dissolved at 5 mg/ml in PBS. The solution was subjected to 10 freeze thaw cycles between liquid nitrogen and a 50 °C water bath. The lipid solution was extruded 21 times through a 100 nm filter. To prepare calcein loaded vesicles, calcein at self-quenching concentrations (70 mM) was added to the phospholipids and after extrusion, the vesicle solution was run through a PD-10 desalting column (GE Healthcare) to separate free calcein from calcein loaded vesicles.

Analyzing Soluble α SN Remaining in Solution

To analyze soluble α SN remaining in the solution, samples were taken from the plate after 24 h incubation and pelleted by centrifugation for 10 min at 21000 g. This speed can pellet large fibrillar aggregates, leaving in the supernatant monomers and oligomers which do not even pellet during ultracentrifugation unless bound to

e.g. phospholipid vesicles (51). We are able to discriminate monomers and oligomers by SDS-PAGE since the latter are SDS-resistant (10). The supernatant was mixed with SDS-PAGE sample loading buffer and heated for 2 min at 95 °C before loading on a 15% SDS-PAGE gel. The supernatant was also run on a Superose 6_10/300 gel filtration column.

Circular Dichroism (CD) Spectroscopy

For far-UV CD, sonicated fibril solutions with protein concentration of 0.2 mg/mL (14 μ M) were placed in a 1 mm cuvette and the spectra were measured from 250 to 195 nm at 25 °C with a Jasco J-810 spectrophotometer (Jasco Spectroscopic Co. Ltd., Japan). To measure the induced changes in the secondary structure of α SN by DMPG vesicles and the effect of olive samples on this interaction, 0.2 mg/mL (14 μ M) of α SN was mixed with 0.2 mg/mL of DMPG vesicles in the presence and absence of 0.15 mg/ml of olive samples in PBS buffer at 37 °C. CD spectra of PBS buffer and the olive solutions were recorded and subtracted from the protein spectra and the CD signal given as mean residue ellipticity (degrees cm² dmol⁻¹).

Transmission Electron Microscopy (TEM)

α SN sample in 5 μ L PBS buffer was transferred to a carbon-coated, glow-discharged 400-mesh grid for 30 s. The grids were washed using 2 drops of double distilled water, stained with 1% (w/v) phosphotungstic acid (pH 6.8), and blotted dry. The samples were viewed in a microscope (JEM-1010; JEOL, Tokyo, Japan) operating at 60 kV. Images were obtained using an Olympus KeenView G2 camera.

Oligomerization Assays

α SN monomer (1 mg/mL) was incubated on an Eppendorf TS-100 thermoshaker (BioSan, Latvia) with 0.15 mg/mL of olive extracts for 1 h at 37 °C and 900 rpm. The solution was centrifuged (21000 g, 20 min) and the supernatant was injected into a 24 mL Superose 6 10/300 gel filtration column at 0.5 mL/min. Samples from both oligomerization and disaggregation assays were run on an SEC-MALS system (Wyatt Technology Europe) using separation on a Superose 6_10/300 gel filtration column and analyzed using 18-angle static laser light

scattering (Dawn Heleos II), refractive index (Optilab T-rEX differential refractometer) and absorbance at 280 nm (Agilent 1260 Analytical UV cell). Data was collected and analysed using the software ASTRA 6.1.7.17 (Wyatt Technology Europe).

Calcein Release Assays

The membrane permeabilization assay was carried out to compare the membrane-disrupting ability of different α SN aggregates that form in the presence and absence of the extracts. Oligomers permeabilize the membrane (and by inference induce toxicity in cells) much more efficiently than fibrils. Permeabilization of vesicles due to the interaction with oligomers results in calcein release and an increase in the fluorescence signal due to dilution. Calcein-loaded DOPG vesicles at a final lipid concentration of 42 μ M were loaded in triplicate in a 140 μ L assay solution onto a 96-well plate (Nunc, Thermo Fisher Scientific, Roskilde, Denmark). The background fluorescence at excitation 485 nm and emission at 520 nm was measured on Genios Pro fluorescence plate reader (Tecan, Mänerdorf, Switzerland) before and after addition of vesicles. The olive extracts and/or oligomers at a final concentration of 0.02–0.2 mg/mL and 0.5 μ M, respectively, were mixed with vesicles in a final volume of 150 μ L. The plates were sealed with crystal clear sealing tape (Hampton Research, Aliso Viejo, CA, USA) and calcein release was measured for 1 h at 37 °C every 1.5 min with 2-s autoshake before each reading. Finally, 1 μ L Triton X-100 (0.1% (w/v)) was added to lyse vesicles, leading to complete calcein release and maximal fluorescence signal. Background fluorescence was subtracted.

HPLC Analysis of Phenolic Compounds in Different Olive Fruit Extracts

The extracts were analyzed with an Ultimate 3000 model HPLC, run on a RP-C18 Luna column, 4.6 mm id \times 250 mm and particle size 5 μ m (Phenomenex, UK). For each injection (50 μ L), elution was performed at a flow rate of 1 mL/min, using a solvent system of water/TFA (1%) (A) and acetic acid/TFA (1 %) (B). Elution was started with 5 % B, and continued with a gradient to 35 % B at 45 min, 90 % B at 55 to 57

min and then reduced to 5 % B at 61 min. Chromatograms were recorded at 230 nm.

Fractionation of Koroneiki Extracts by HPLC

Dried extracts were reconstituted using 1.75 mL of water. Fractionation was carried out using an HPLC system (Dionex UltiMate 3000, Thermo Fisher Scientific) equipped with an Ascentis C-18 column (5 μ m, 5 \times 250 mm, Supelco, UK). Chromatographic separation was performed using a constant flow rate of 1 mL/min of the mobile phases water/0.1% formic acid (A) and acetonitrile/0.1% formic acid (B). The binary gradient was: 0–10 min, 5% B; 10–50 min, 22% B; 50–60 min, 37% B; and finally 60–70 min, 50% B. Fractions were collected every 2.5 min between 5 and 70 min (T1–T26). Twelve injections (100 μ L each) were performed and fractions from repeated runs were combined. Thirty μ L of each fraction was diluted with 270 μ L of 80/20 (v/v) water/methanol and subsequently analysed by uHPLC-MS. The remainder of each fraction was dried using a Speedvac concentrator (Genevac, Suffolk, UK).

Identification of Phenolic Compounds in Koroneiki Extract Fractions by uHPLC-MS

To identify the compounds, Ultra High Performance Liquid Chromatography-Mass Spectrometry (uHPLC-MS) were recorded with an Ultimate 3000 RS uHPLC system, equipped with a DAD-3000 photodiode array detector, coupled to an LTQ-Orbitrap Elite mass spectrometer (Thermo Scientific, Germany). An injection volume of 10 μ L was used and the elution was performed on a reversed-phase C18 Hypersil gold column (1.9 μ m, 30 \times 2.1 mm i.d., Thermo, Hemel Hempstead, UK), at 35 °C, using a solvent system consisting of water/0.1% formic acid (A) and acetonitrile/0.1% formic acid (B) under the following conditions: 0–5 min, 0% B; 5–27 min, 31.6% B; 27–34 min, 45% B; 34–37.5 min, 75% B at a flow rate of 0.3 mL/min. Mass spectra were collected using an LTQ-Orbitrap Elite with a heated ESI source (Thermo Scientific, Germany). Mass spectra were acquired in negative mode with a resolution of 120,000 over m/z 50–1500. The source voltage, sheath gas, auxiliary gas, sweep gas and capillary temperature were set to 2.5 kV, 35 (arbitrary units), 10 (arbitrary units), 0.0 (arbitrary units)

and 350 °C respectively. Default values were used for other acquisition parameters. Automatic MS-MS was performed on the 4 most abundant ions using an isolation width of m/z 2. Ions were fragmented using high-energy C-trap dissociation (HCD) with a normalized collision energy of 65 and an activation time of 0.1 ms. Data analysis was carried out using Xcalibur v. 2.2 (Thermo Scientific, Germany). Compounds were identified on the basis of their retention time, accurate mass and MSMS fragmentation patterns. Where possible, known compounds were compared to authentic standards if available. Where this was not possible, a comparison to the reported MSMS fragmentation data was made for known compounds. Compounds where structural data could not be verified were labelled as unknown. A full table of the LC-MS data was prepared, including details of identification method for each component and reference data for known compounds (Table S2).

Antioxidant Activity

The antioxidant activity of the olive extracts was determined by monitoring the disappearance of DPPH• in the presence of olive extracts at 517 nm. Olive extracts (20 µl) at various concentrations was mixed with 200 µl of DPPH• solution (0.135 mM). The resulting medium was incubated at room temperature in darkness for 30 min. The antioxidant activity was determined using the following formula:

$$\text{Antioxidant activity} = \frac{(\text{Abs}_{517}^{\text{control}} - \text{Abs}_{517}^{\text{sample}}) / \text{Abs}_{517}^{\text{control}} \times 100}{(4)} \quad (4)$$

ROS assay

To assess whether olive extracts interfered with the level of ROS within the cells, 2', 7'-dichlorodihydrofluorescein diacetate (DCFH-DA) was used. OLN 93 cells were seeded in 96-well plates at a density of 6×10^4 cells/mL and incubated in a humidified atmosphere incubator at 37°C for 24 h. The medium was then removed and the cells washed with PBS and replaced by PBS containing 15 µM DCFH-DA. The plate was incubated for 45 min in the dark in a CO₂ incubator. DCFH-DA was removed and the wells were washed with PBS, treated with culture medium containing olive extracts in the absence or presence of 100 µM H₂O₂ and incubated at 37°C (for 1 h) after which fluorescence of DCF

was recorded in a microtiter plate reader (excitation / emission: 490/527 nm).

Evaluation of Cell Viability

The 3-[4, 5-dimethylthiazol-2-yl]-2,5-diphenyltetrazolium bromide (MTT) assay was implemented to measure cellular viability after 24 h treatment by monomeric or aggregated forms of α SN. OLN-93 and SH-SY5Y cells were seeded in 96-well plates at a concentration of 30×10^3 and 60×10^3 cells/mL, respectively, in Dulbecco's Modified Eagle Medium (DMEM) supplemented with 10 % (v/v) fetal bovine serum (FBS), 100 units/mL penicillin, and 100 µg/mL streptomycin and cultured for 24 h. The medium was then replaced with fresh medium containing different concentrations of olive extracts or with 12.5 % α SN samples (collected during the fibrillation process). After 24 h at 37 °C, the old medium was replaced with fresh medium containing 10 % MTT (5 mg/mL), and the plates were incubated for an additional 4 h at 37 °C. To avoid possible interference between antioxidant compounds and the MTT assay, the cells were washed to remove aggregates and compounds before adding MTT. The formazan crystals were dissolved in 100 µL DMSO by incubating for 1 h on a shaking table at room temperature. Finally, absorbance was determined by a plate reader at 570 nm using 650 nm as a reference wavelength. Cell viability was calculated as follows:

$$\text{Cell viability (\%)} = \frac{\text{Abs}_{570} (\text{Treated cells})}{\text{Abs}_{570} (\text{Control cells})} \times 100 \quad (5)$$

LDH Assay

Release of cytoplasmic enzyme, lactate dehydrogenase (LDH), as the sign of loss of membrane integrity was measured. After the treatment of the cells with α SN samples, 100 µL of growth medium was added to 1 ml of the kit substrate and absorbance at 340 nm was determined for 4 min to follow the conversion of NADH to NAD⁺. The values were expressed as a percentage of the untreated cells as control.

Analysis of HPLC Elution Profiles

The average values of the end ThT values of α SN aggregation in the presence of different concentrations of olive extracts and HPLC data of the olive extracts were used to analyze the effect of different compounds in the olive fruit extracts.

The “peakutils” Python package (<https://bitbucket.org/lucashnegri/peakutils>) was used to identify peaks in the HPLC data and the “sklearn” Python package (<http://scikit-learn.org/stable/>) to cluster them as follows:

- a. The threshold for identifying peaks (the minimum height) was set to 750 A.U.
- b. The minimum distance between peaks was set to 50 data points.
- c. All of the peaks identified in this way (across all of the datasets) were compiled into a single list of peaks, and a k-means clustering was used to cluster the peaks into 5 groups.
- d. The cluster centers were extracted and used to identify the peaks in further analyses.

For each peak that was identified, a relative measure of the “amount of compound” in each sample was determined by multiplying the concentration of the extract (mg/mL) by the height of the peak. Where the data was available, the “amount of compound” was plotted against the ThT signal. Data points with ThT signals below 1000 (arbitrary unit) were excluded from further analysis under the assumption that these corresponded to maximal inhibition and therefore might obscure attempts to determine whether the concentration of the compound was related to the level of the ThT signal in the relevant range (between 7000 and 1000 units). For each compound, the coefficient of determination (R^2),

and Spearman’s rank correlation coefficient were computed, and an isotonic regression model was built from the data. The R^2 value measures the goodness of fit assuming a linear model, while the Spearman’s rank correlation coefficient measures how monotonically related the two quantities are without making an assumption about the functional form of the relation. R-squared values are always positive and between 0 and 1. Spearman R values can be in the range of -1 to 1. The isotonic regression generates an optimal monotonic fit to the data. The slope of the optimal linear fit (the m-value) was taken a measure of potency, with larger (negative) slopes corresponding to more potent inhibition. Finally, a correlation analysis was performed to determine which peaks had correlated amounts across all of the samples.

Statistical Analysis

Data were obtained in triplicate and averaged. The results are shown as mean \pm standard deviation (SD). Statistical differences between group means were analyzed by analysis of variance (ANOVA). A value of $p < 0.05$ was considered statistically significant.

ACKNOWLEDGEMENTS

H.M.B., F.A., and D.M were supported by the grant 982 from Center for International Scientific Studies & Collaboration (CISSC). H.E., N.P.S., C.S., I.M.M., G.C., and D.E.O. were supported by grant 4005-00082 from the Independent Research Fund Denmark | Technology and Production. C.L., A.T., and J.L.W were supported by a grant that Rothamsted Research received from the Biotechnology and Biological Sciences Research Council (BBSRC) of the UK. J.W. received funding from the Tailoring Plant Metabolism Institute Strategic Programme grant [BB/E/C/000I0410], funded by the BBSRC.

CONFLICT OF INTEREST

The authors declare that they have no conflicts of interest with the contents of this article.

References

1. Hardy, J., Cookson, M. R., and Singleton, A. (2003) Genes and parkinsonism. *The Lancet Neurology* **2**, 221–228
2. Spillantini, M. G., Schmidt, M. L., Lee, V. M.-Y., Trojanowski, J. Q., Jakes, R., and Goedert, M. (1997) alpha-Synuclein in Lewy bodies. *Nature* **388**, 839–840
3. Jakes, R., Spillantini, M. G., and Goedert, M. (1994) Identification of two distinct synucleins from human brain. *FEBS letters* **345**, 27–32

4. Masuda-Suzukake, M., Nonaka, T., Hosokawa, M., Oikawa, T., Arai, T., Akiyama, H., Mann, D. M., and Hasegawa, M. (2013) Prion-like spreading of pathological α -synuclein in brain. *Brain* **136**, 1128–1138
5. Van Rooijen, B., van Leijenhorst-Groener, K., Claessens, M., and Subramaniam, V. (2009) Tryptophan fluorescence reveals structural features of α -synuclein oligomers. *Journal of molecular biology* **394**, 826–833
6. Fauvet, B., Mbefo, M. K., Fares, M.-B., Desobry, C., Michael, S., Ardah, M. T., Tsika, E., Coune, P., Prudent, M., Lion, N., and others (2012) α -Synuclein in central nervous system and from erythrocytes, mammalian cells, and *Escherichia coli* exists predominantly as disordered monomer. *Journal of Biological Chemistry* **287**, 15345–15364
7. Paslawski, W., Mysling, S., Thomsen, K., Jørgensen, T. J., and Otzen, D. E. (2014) Co-existence of Two Different α -Synuclein Oligomers with Different Core Structures Determined by Hydrogen/Deuterium Exchange Mass Spectrometry. *Angewandte Chemie International Edition* **53**, 7560–7563
8. Ingelsson, M. (2016) Alpha-Synuclein Oligomers - Neurotoxic Molecules in Parkinson's Disease and Other Lewy Body Disorders. *Frontiers in neuroscience* **10**, 408
9. Fink, A. L. (2006) in *Misbehaving Proteins* pp. 265–285, Springer
10. Paslawski, W., Andreasen, M., Nielsen, S. B., Lorenzen, N., Thomsen, K., Kaspersen, J. D., Pedersen, J. S., and Otzen, D. E. (2014) High Stability and Cooperative Unfolding of α -Synuclein Oligomers. *Biochemistry* **53**, 6252–6263
11. Prots, I., Veber, V., Brey, S., Campioni, S., Buder, K., Riek, R., Böhm, K. J., and Winner, B. (2013) α -Synuclein oligomers impair neuronal microtubule-kinesin interplay. *Journal of Biological Chemistry* **288**, 21742–21754
12. Chen, L., Jin, J., Davis, J., Zhou, Y., Wang, Y., Liu, J., Lockhart, P. J., and Zhang, J. (2007) Oligomeric α -synuclein inhibits tubulin polymerization. *Biochemical and biophysical research communications* **356**, 548–553
13. Nakamura, K. (2013) α -Synuclein and mitochondria: partners in crime? *Neurotherapeutics* **10**, 391–399
14. Nakamura, K., Nemani, V. M., Azarbal, F., Skibinski, G., Levy, J. M., Egami, K., Munishkina, L., Zhang, J., Gardner, B., Wakabayashi, J., and others (2011) Direct membrane association drives mitochondrial fission by the Parkinson disease-associated protein α -synuclein. *Journal of Biological Chemistry* **286**, 20710–20726
15. Angelova, P. R., and Abramov, A. Y. (2018) Role of mitochondrial ROS in the brain: from physiology to neurodegeneration. *FEBS letters* **592**, 692–702
16. Lorenzen, N., Nielsen, S. B., Yoshimura, Y., Vad, B. S., Andersen, C. B., Betzer, C., Kaspersen, J. D., Christiansen, G., Pedersen, J. S., Jensen, P. H., and others (2014) How epigallocatechin gallate can inhibit α -synuclein oligomer toxicity in vitro. *Journal of Biological Chemistry* **289**, 21299–21310
17. Keys, A., Mienotti, A., Karvonen, M. J., Aravanis, C., Blackburn, H., Buzina, R., Djordjevic, B., Dontas, A., Fidanza, F., Keys, M. H., and others (1986) The diet and 15-year death rate in the seven countries study. *American journal of epidemiology* **124**, 903–915
18. Gaskins, A. J., Rovner, A. J., Mumford, S. L., Yeung, E., Browne, R. W., Trevisan, M., Perkins, N. J., Wactawski-Wende, J., Schisterman, E. F., and Group, B. S. (2010) Adherence to a Mediterranean diet and plasma concentrations of lipid peroxidation in premenopausal women-. *The American journal of clinical nutrition* **92**, 1461–1467

19. Dai, J., Jones, D. P., Goldberg, J., Ziegler, T. R., Bostick, R. M., Wilson, P. W., Manatunga, A. K., Shallenberger, L., Jones, L., and Vaccarino, V. (2008) Association between adherence to the Mediterranean diet and oxidative stress-. *The American journal of clinical nutrition* **88**, 1364–1370
20. Casamenti, F., and Stefani, M. (2016) Olive polyphenols: new promising agents to combat aging-associated neurodegeneration. *Expert Review of Neurotherapeutics*, 1–14
21. Tripoli, E., Giammanco, M., Tabacchi, G., Di Majo, D., Giammanco, S., and La Guardia, M. (2005) The phenolic compounds of olive oil: structure, biological activity and beneficial effects on human health. *Nutrition research reviews* **18**, 98–112
22. Rigacci, S., Guidotti, V., Bucciantini, M., Nichino, D., Relini, A., Berti, A., and Stefani, M. (2011) Abeta (1-42) aggregates into non-toxic amyloid assemblies in the presence of the natural polyphenol oleuropein aglycon. *Current Alzheimer Research* **8**, 841–852
23. Daccache, A., Lion, C., Sibille, N., Gerard, M., Slomianny, C., Lippens, G., and Cotelle, P. (2011) Oleuropein and derivatives from olives as Tau aggregation inhibitors. *Neurochemistry international* **58**, 700–707
24. Caruana, M., Högen, T., Levin, J., Hillmer, A., Giese, A., and Vassallo, N. (2011) Inhibition and disaggregation of α -synuclein oligomers by natural polyphenolic compounds. *FEBS letters* **585**, 1113–1120
25. Ahmad, E., Ahmad, A., Singh, S., Arshad, M., Khan, A. H., and Khan, R. H. (2011) A mechanistic approach for islet amyloid polypeptide aggregation to develop anti-amyloidogenic agents for type-2 diabetes. *Biochimie* **93**, 793–805
26. Wu, C., Lei, H., Wang, Z., Zhang, W., and Duan, Y. (2006) Phenol red interacts with the protofibril-like oligomers of an amyloidogenic hexapeptide NFGAIL through both hydrophobic and aromatic contacts. *Biophysical journal* **91**, 3664–3672
27. Palazzi, L., Bruzzone, E., Bisello, G., Leri, M., Stefani, M., Bucciantini, M., and de Laureto, P. P. (2018) Oleuropein aglycone stabilizes the monomeric α -synuclein and favours the growth of non-toxic aggregates. *Scientific reports* **8**, 8337
28. Omar, S. H., Scott, C. J., Hamlin, A. S., and Obied, H. K. (2018) Biophenols: Enzymes (Abeta-secretase, Cholinesterases, histone deacetylase and tyrosinase) inhibitors from olive (*Olea europaea* L.). *Fitoterapia* **128**, 118–129
29. Servili, M., and Montedoro, G. (2002) Contribution of phenolic compounds to virgin olive oil quality. *European Journal of Lipid Science and Technology* **104**, 602–613
30. Petridis, A., Therios, I., and Samouris, G. (2012) Genotypic variation of total phenol and Oleuropein concentration and antioxidant activity of 11 Greek olive cultivars (*Olea europaea* L.). *HortScience* **47**, 339–342
31. Romero, C., Medina, E., Mateo, M. A., and Brenes, M. (2017) Quantification of bioactive compounds in Picual and Arbequina olive leaves and fruit. *Journal of the Science of Food and Agriculture* **97**, 1725–1732
32. Vossen, P. (2007) Olive oil: history, production, and characteristics of the world's classic oils. *HortScience* **42**, 1093–1100
33. Giehm, L., and Otzen, D. E. (2010) Strategies to increase the reproducibility of protein fibrillization in plate reader assays. *Analytical biochemistry* **400**, 270–281
34. Lorenzen, N., Nielsen, S. B., Buell, A. K., Kaspersen, J. D., Arosio, P., Vad, B. S., Paslawski, W., Christiansen, G., Valnickova-Hansen, Z., Andreasen, M., and others (2014) The role of stable α -synuclein oligomers in the molecular events underlying amyloid formation. *Journal of the American Chemical Society* **136**, 3859–3868

35. Kjaer, L., Giehm, L., Heimburg, T., and Otzen, D. (2009) The Influence of Vesicle Size and Composition on α -Synuclein Structure and Stability. *Biophysical journal* **96**, 2857–2870
36. Perni, M., Galvagnion, C., Maltsev, A., Meisl, G., Müller, M. B., Challa, P. K., Kirkegaard, J. B., Flagmeier, P., Cohen, S. I., Cascella, R., and others (2017) A natural product inhibits the initiation of α -synuclein aggregation and suppresses its toxicity. *Proceedings of the National Academy of Sciences* **114**, E1009–E1017
37. Aliakbari, F., Shabani, A., Bardania, H., Seyedi, E., Alsadat, H., Mohammad-Beigi, H., Tayaranian Marvian, A., Nassoti, M., Vafaei, A. A., Shojaosadati, S. A., and others (2017) Neurotoxicity of pre-incubated alpha-synuclein with neutral nanoliposomes on PC12 and SHSY5Y cell lines. *Scientia Iranica* **24**, 3542–3553
38. Zhao, J., Liang, Q., Sun, Q., Chen, C., Xu, L., Ding, Y., and Zhou, P. (2017) (-)-Epigallocatechin-3-gallate (EGCG) inhibits fibrillation, disaggregates amyloid fibrils of α -synuclein, and protects PC12 cells against α -synuclein-induced toxicity. *Rsc Advances* **7**, 32508–32517
39. Vossen, P. M. (2007) *Organic olive production manual*, UCANR Publications
40. Mohammad-Beigi, H., Morshedi, D., Shojaosadati, S. A., Pedersen, J. N., Marvian, A. T., Aliakbari, F., Christiansen, G., Pedersen, J. S., and Otzen, D. E. (2016) Gallic acid loaded onto polyethylenimine-coated human serum albumin nanoparticles (PEI-HSA-GA NPs) stabilizes α -synuclein in the unfolded conformation and inhibits aggregation. *Rsc Advances* **6**, 85312–85323
41. Souza, J. M., Giasson, B. I., Chen, Q., Lee, V. M.-Y., and Ischiropoulos, H. (2000) Dityrosine Cross-linking Promotes Formation of Stable α -Synuclein Polymers Implication Of Nitrate And Oxidative Stress In The Pathogenesis Of Neurodegenerative Synucleinopathies. *Journal of Biological Chemistry* **275**, 18344–18349
42. Abou-Sleiman, P. M., Muqit, M. M., and Wood, N. W. (2006) Expanding insights of mitochondrial dysfunction in Parkinson's disease. *Nature Reviews Neuroscience* **7**, 207
43. Mandel, S., and Youdim, M. B. (2004) Catechin polyphenols: neurodegeneration and neuroprotection in neurodegenerative diseases. *Free radical biology and medicine* **37**, 304–317
44. Diomedea, L., Rigacci, S., Romeo, M., Stefani, M., and Salmona, M. (2013) Oleuropein aglycone protects transgenic *C. elegans* strains expressing Abeta42 by reducing plaque load and motor deficit. *PLoS one* **8**, e58893
45. Rigacci, S., Guidotti, V., Bucciantini, M., Parri, M., Nediani, C., Cerbai, E., Stefani, M., and Berti, A. (2010) Oleuropein aglycon prevents cytotoxic amyloid aggregation of human amylin. *The Journal of nutritional biochemistry* **21**, 726–735
46. Hosseini-Mazinani, M., Torkzaban, B., and Arab, J. (2013) Iranian Olive Catalogue: Morphological and Molecular Characterization of Iranian Olive Germplasm. *Tehran: NIGEB*
47. Amiri-Nowdijeh, A., Fazelipour, F., Haghbeen, K., Taheri, M., and others (2018) Minor Olive Varieties from Iran with Promising Nutraceutical Properties. *Journal of Agricultural Science and Technology* **20**, 347–357
48. Mohammad-Beigi, H., Shojaosadati, S. A., Marvian, A. T., Pedersen, J. N., Klausen, L. H., Christiansen, G., Pedersen, J. S., Dong, M., Morshedi, D., and Otzen, D. E. (2015) Strong interactions with polyethylenimine-coated human serum albumin nanoparticles (PEI-HSA

- NPs) alter alpha-synuclein conformation and aggregation kinetics. *Nanoscale* **7**, 19627–19640
49. Morris, A. M., Watzky, M. A., Agar, J. N., and Finke, R. G. (2008) Fitting neurological protein aggregation kinetic data via a 2-step, minimal “Ockham’s razor” model: the Finke-Watzky mechanism of nucleation followed by autocatalytic surface growth. *Biochemistry* **47**, 2413–2427
 50. Nesgaard, L., Vad, B., Christiansen, G., and Otzen, D. (2009) Kinetic partitioning between aggregation and vesicle permeabilization by modified ADan. *Biochimica et Biophysica Acta (BBA)-Proteins and Proteomics* **1794**, 84–93
 51. Sahin, C., Lorenzen, N., Lemminger, L., Christiansen, G., Møller, I. M., Vesterager, L. B., Pedersen, L. Ostergaard, Fog, K., Kallunki, P., and Otzen, D. E. (2017) Antibodies against the C-terminus of α -synuclein modulate its fibrillation. *Biophysical chemistry* **220**, 34–41

Table 1. For each olive extract constituent, coefficient of determination (R^2), the slope of the optimal linear fit (m-value) and Spearman's rank correlation coefficient for each compound.

Peak elution time	Compound	R-Squared ^a	m-value ^b	Spearman R ^c
35.5	Oleuropein	0.29	-11.76	-0.73
28.5	Verbascoside	0.39	-24.69	-0.71
50.3	Oleuropein aglycon	0.48	-88.31	-0.76
40.0	Hydroxyoleuropein aglycone	0.24	-24.13	-0.72

^a Coefficient of determination: measures the goodness of fit assuming a linear model.

^b The slope of the optimal linear fit (the m-value): measures the potency with larger (negative) slopes corresponding to more potent inhibition.

^c Spearman's rank correlation coefficient: measures how monotonically related the two quantities are without making an assumption about the functional form of the relation.

Table 2. Ranking of the top 7 olive variety extracts in different assays.

Assay	T10	T17	T20	T23	T24	Rowghani	Koroneiki	Ref.
Inhibiting aggregation ^a	++++	++	+++	++	+++	++++	++++	Fig. 1
Inhibiting secondary nucleation ^b	++++	+++	++++	++	+++	+++	++++	Fig. 3
Formation of small oligomers ^c	+++	+++	++	++	++	++	++++	Fig. 3
Formation of large oligomers ^d	++	++	+	++++	++	+++	+	Fig. 3
Inducing formation of less toxic aggregates to SH-SY5Y cells during fibrillation ^e	++++	++++	+++	+++	+++	++++	++++	Fig. 4

^a at 0.1 mg/ml of the olive extracts, + denotes 0-25 % inhibition, ++ 25-50 % inhibition, +++ 50-75 % inhibition, and ++++ 75-100 % inhibition.

^b at 0.15 mg/ml of the olive extracts, + denotes 0-25 % inhibition, ++ 25-50 % inhibition, +++ 50-75 % inhibition, and ++++ 75-100 % inhibition.

^c at 0.15 mg/ml of the olive extracts, Min [small oligomer] = A, Max [small oligomer] = B, $x = \frac{A-B}{4}$.

+ denotes $A < [\text{small oligomer}] < A+x$, ++ denotes $A+x < [\text{small oligomer}] < A+2x$, +++ denotes $A+2x < [\text{small oligomer}] < A+3x$, and ++++ denotes $A+3x < [\text{small oligomer}] < B$.

^d The same formula for ranking as in note c, this time using the large oligomers.

^e Average of toxicity of aggregates formed over different time ranges compared to control.

Table 3. Ranking of the fractions in different assays.

Assay	5	6	17	18	19	20	21	22	23	24	25	26	Ref.
Inhibiting aggregation ^a	++++	++	++	+++	++++	++++	++++	++++	+++	++++	+++	++	Fig. 6
Inhibiting secondary nucleation ^b	++++	++++	++	++	++++	++++	++++	++++	++	++	++	++	Fig. 6
Formation of small oligomers ^c	++	+++	++	++++	+++	+++	++++	++++	+++	++	++	++	Fig. S11
Inducing formation of less toxic aggregates to SH-SY5Y cells during fibrillation ^d	++++	+++	++++	++++	++++	++++	++++	++++	++++	++++	++++	++++	Fig. 6

^a at 0.1 mg/ml of the olive extracts, + denotes 0-25 % inhibition, ++ 25-50 % inhibition, +++ 50-75 % inhibition, and +++++ 75-100 % inhibition.

^b at 0.15 mg/ml of the olive extracts, + denotes 0-25 % inhibition, ++ 25-50 % inhibition, +++ 50-75 % inhibition, and +++++ 75-100 % inhibition.

^c at 0.15 mg/ml of the olive extracts, Min [small oligomer] = A, Max [small oligomer] = B, $x = \frac{A-B}{4}$.

+ denotes $A < [\text{small oligomer}] < A+x$, ++ denotes $A+x < [\text{small oligomer}] < A+2x$, +++ denotes $A+2x < [\text{small oligomer}] < A+3x$, and +++++ denotes $A+3x < [\text{small oligomer}] < B$.

^d Average of toxicity of aggregates formed over different time ranges compared to control.

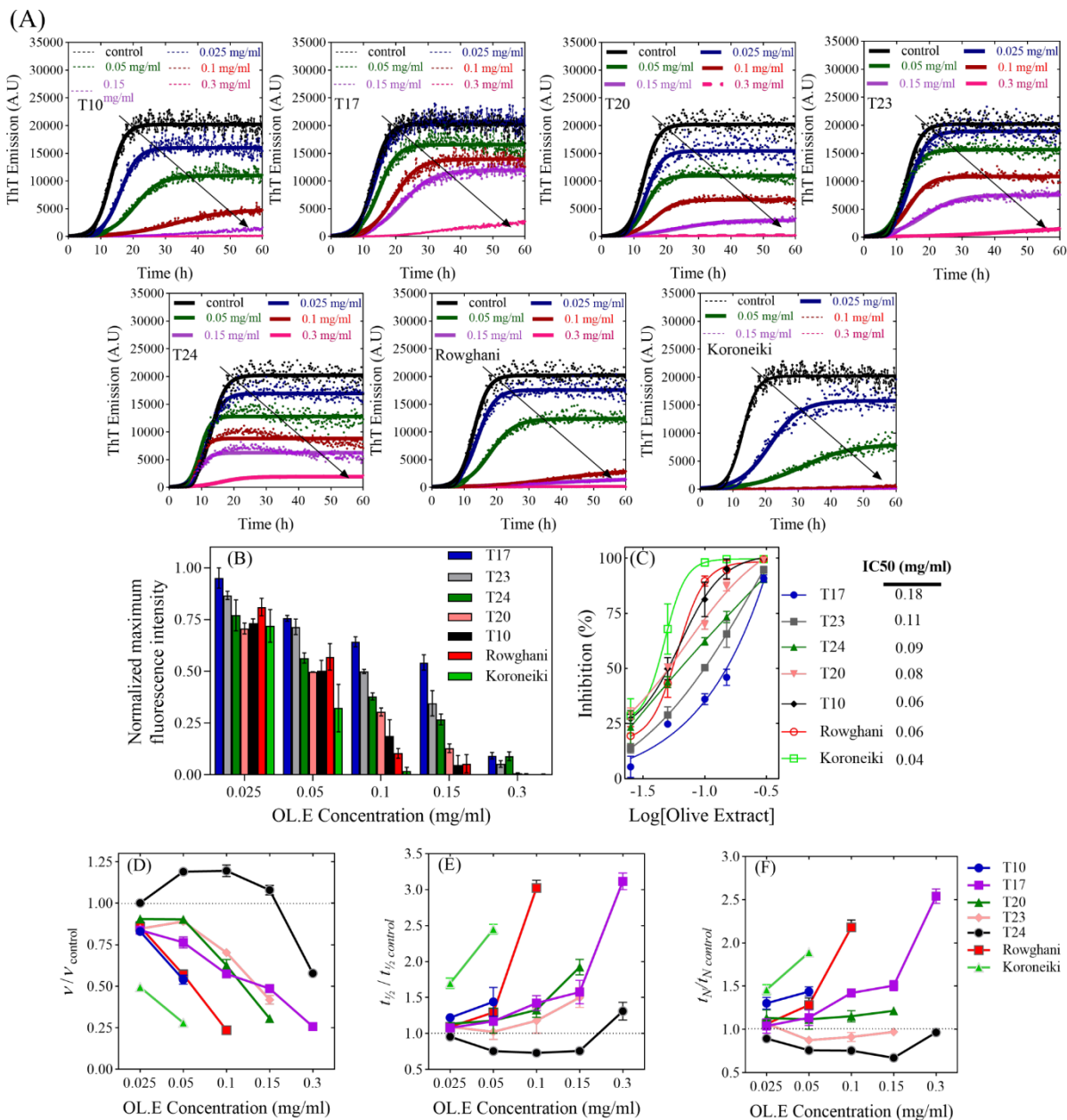
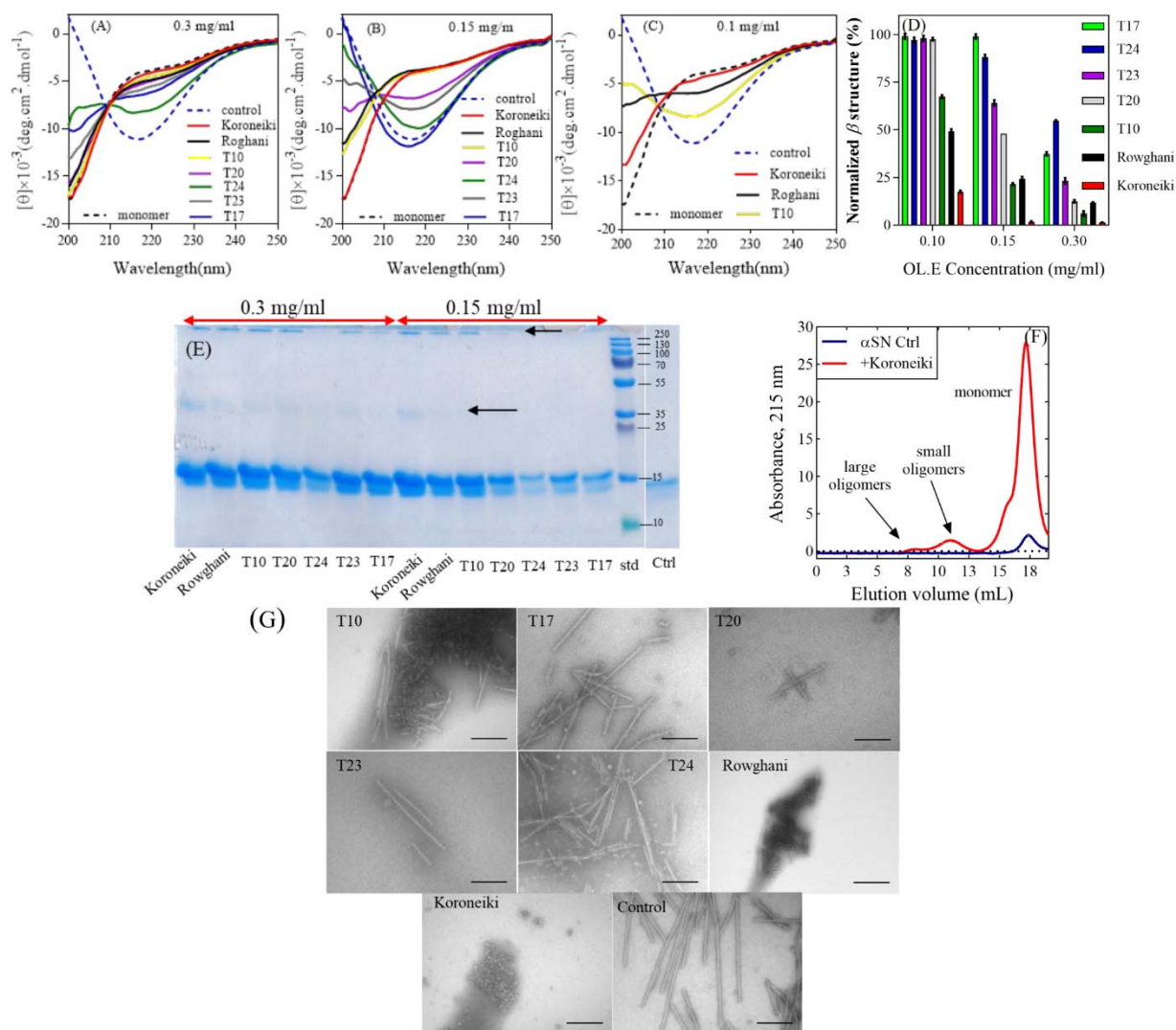


Fig. 1. The effect of the extracts on α SN fibrillation. (A) The effect of 0-0.3 mg/ml of the olive extracts on the kinetics of α SN fibrillation at 5 different concentrations monitored by ThT fluorescence. Joined lines show Finke-Watzky model fitted to the experimental data. (B) The effect of the selected extracts (7 out of 15 extracts) at different concentrations (0.025, 0.05, 0.1, 0.15, and 0.3 mg/ml) on the maximum ThT fluorescence intensity. (C) ThT end-point levels are converted to % inhibition and fitted to Eq. 1 to calculate the IC_{50} of the extracts. (D-F) Kinetic parameters for α SN fibrillation as a function of various concentration of the extracts relative to the values in the absence of the extracts ((D) relative growth rate ($v/v_{control}$), (E) relative half time ($t_{1/2}/t_{1/2, control}$), and (F) relative lag time ($t_N/t_{N, control}$)).



Sample	Average Length of fibrils (μ m)	Number of fibrils measured	Comments
α SN+T10	0.37 ± 0.087	10	small unstructured aggregates + few fibrils
α SN+T17	0.33 ± 0.19	25	few fibrils with broad size distribution
α SN+T20	0.2 ± 0.053	10	very few small fibrils
α SN+T23	0.32 ± 0.081	10	very few small fibrils
α SN+T24	0.5 ± 0.12	28	few fibrils with broad size distribution
α SN+Rowghani	None detected	0	small aggregates without any fibrils
α SN+Koroneiki	None detected	0	small aggregates without any fibrils
α SN Control	0.68 ± 0.092	40	large homogeneous fibrils everywhere on the grid

Fig. 2. Far-UV CD spectra of α SN incubated alone (control) and in the presence of (A) 0.3 mg/ml, (B) 0.15 mg/ml, and (C) 0.1 mg/ml of the 7 selected extracts after 24 h. (D) Normalized β structure (%) of α SN incubated in the presence of the 7 selected extracts. (E) SDS-PAGE analysis of the supernatants of the incubated samples of α SN in the absence and presence of 0.15 and 0.3 mg/ml of the best extracts in inhibiting α SN fibrillation. Monomeric α SN has a molecular weight of 14.5 kDa. Arrows highlight dimers (≈ 35 kDa) and oligomers (> 250 kDa). (F) The SEC-profile of the supernatants of the samples of α SN incubated for 24 h with or without 0.15 mg/ml of Koroneiki extract. (G) Electron microscopy of α SN after 24 h incubation in the absence (control) and presence of 0.3 mg/ml of the 7 selected olive fruit extracts. Scale bar, 200 nm. The size and distribution of the fibrils in each sample are summarized in the table below Fig. 2G. The length of fibrils were obtained in three TEM images for each sample and averaged.

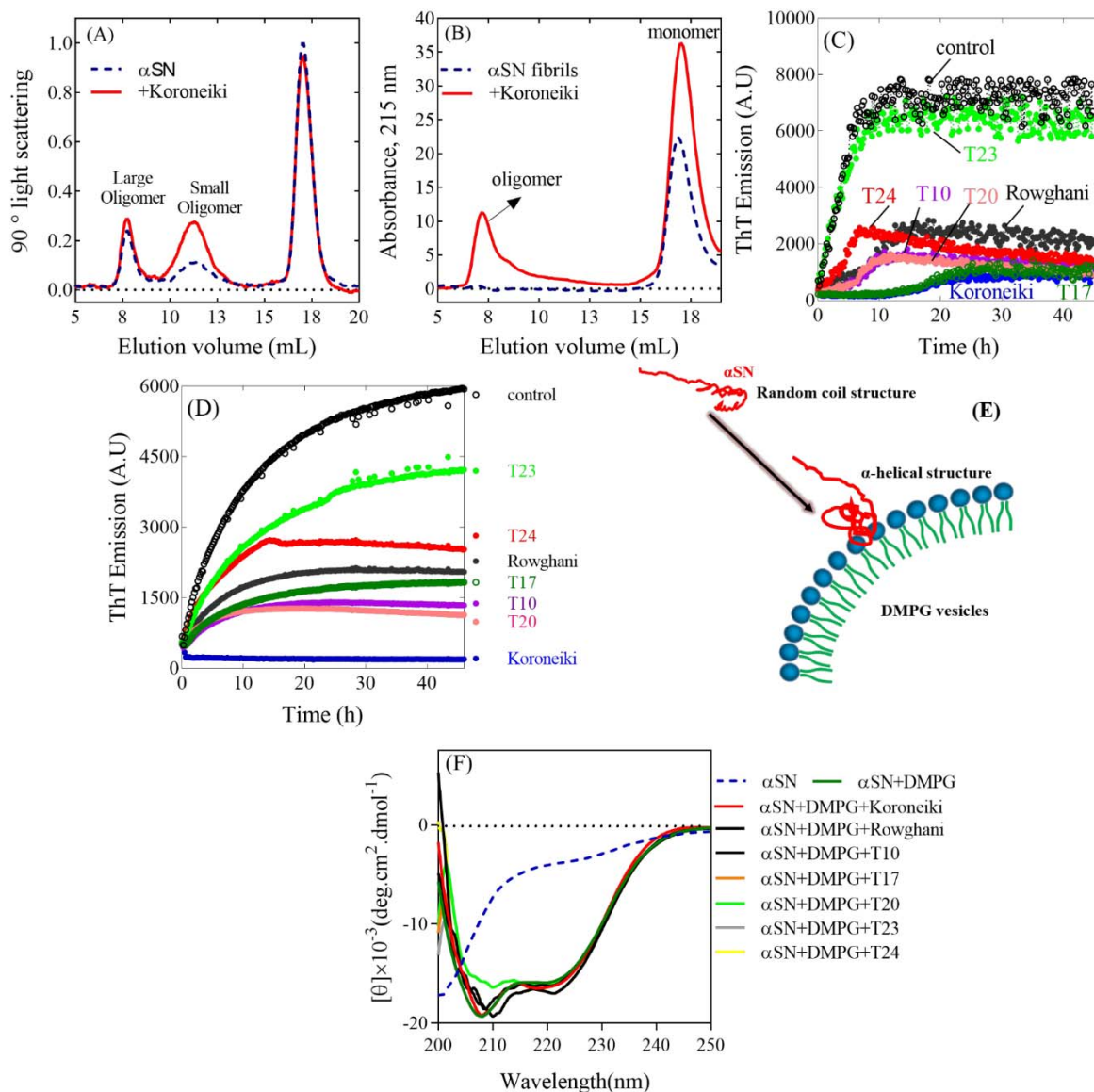


Fig. 3. The SEC-profile of the supernatants of the (A) samples of α SN incubated for 1 h and (B) preformed α SN fibrils preincubated overnight with or without 0.15 mg/ml of Koroneiki extract. The effect of the extracts (0.15 mg/ml) on the seeding of α SN aggregation under (C) shaking and (D) non- shaking condition. (E) Schematic representation of the α -helix structure induced in α SN by DMPG vesicles. (F) The effect of the extracts (0.15 mg/ml) on the interaction of monomer (14 μ M) and DMPG vesicles (0.2 mg/ml).

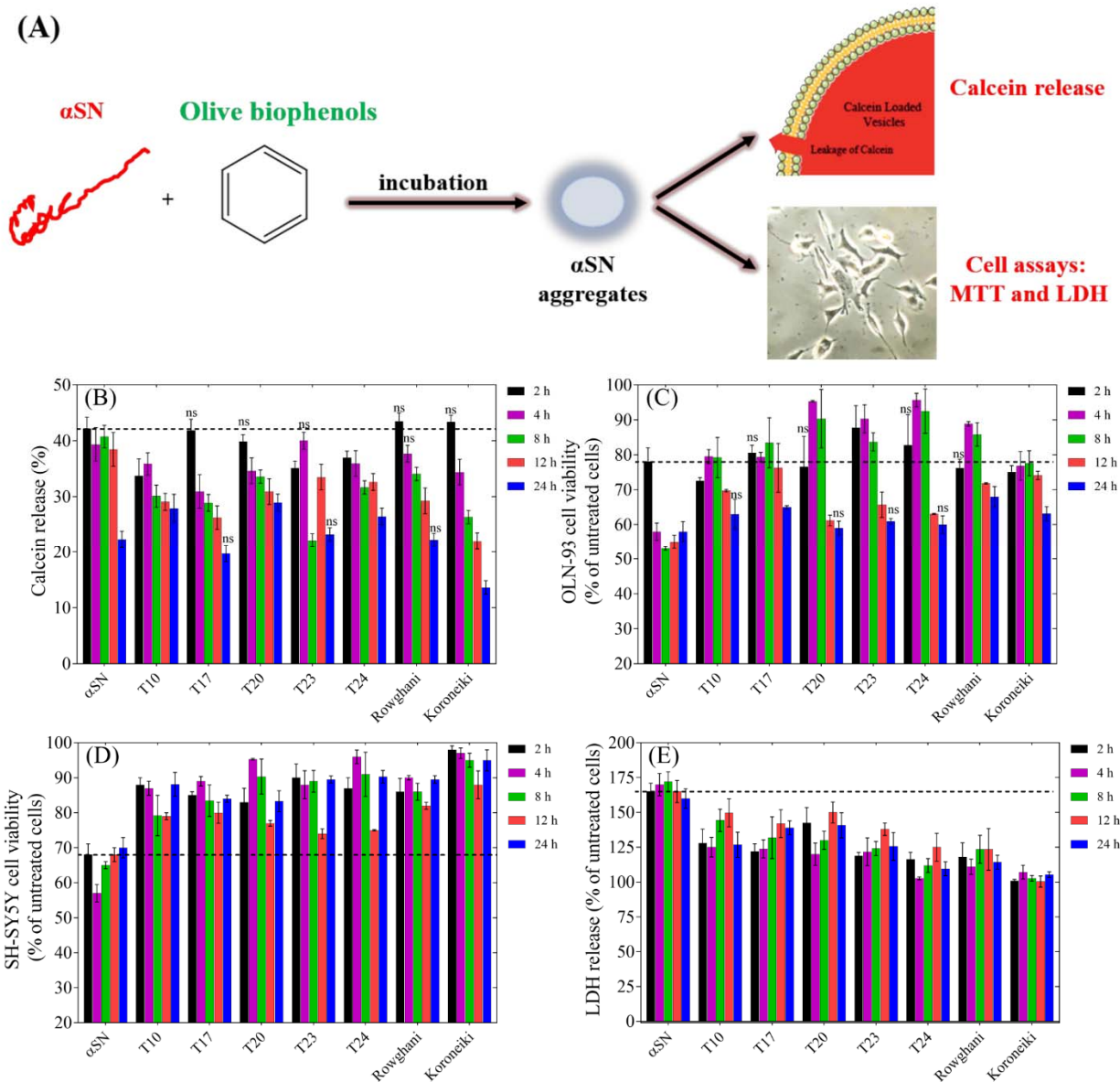


Fig. 4. (A) Schematic representation of the effect of olive variety extracts on the membrane permeabilization and cytotoxicity of α SN aggregates. (B) Calcein release from DOPG vesicles after 20 min incubation with α SN aggregates formed alone and in the presence of the best extracts (0.3 mg/ml) over different times (0-24 h). Viability of (C) OLN-93 and (D) SH-SY5Y cells after 2-24 h incubation with α SN aggregates formed alone and in the presence of the best extracts (0.3 mg/ml) over different times (0-24 h). (E) Cytotoxicity of α SN aggregates to SH-SY5Y cells was assayed by LDH-release. LDH signals were normalized to untreated cells. For all assays, values represent means \pm SD and the differences between the groups and α SN control are significant ($P < 0.05$) unless marked "ns".

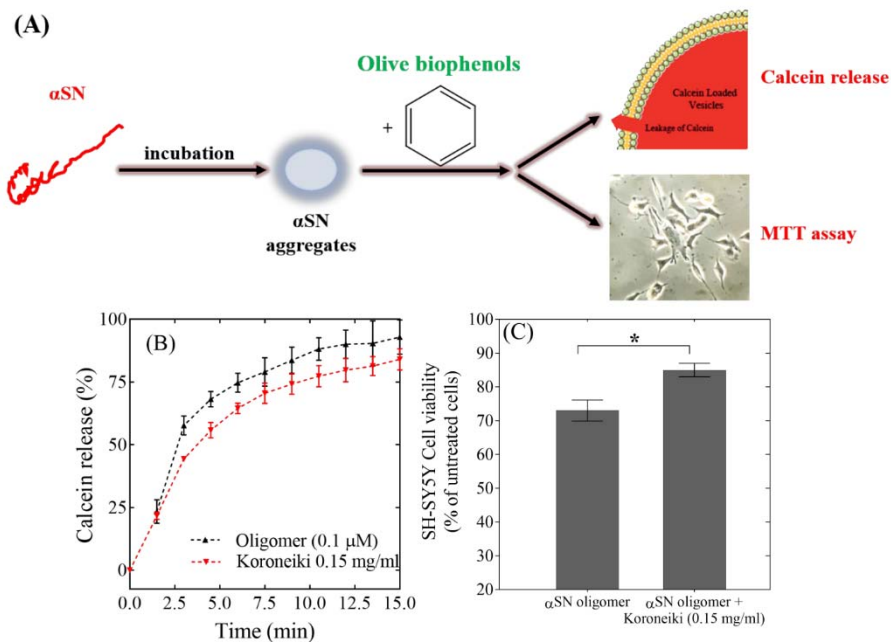


Fig. 5. (A) Schematic representation of the effect of Koroneiki extract fractions on the membrane permebilization and cytotoxicity of α SN aggregates. (B) Calcein release from DOPG vesicles induced by oligomers (0.1 μ M) either alone or in the presence of Koroneiki (0.2 mg/ml). The Koroneiki extract is used at the highest concentration at which quenching of fluorescence does not happen. (C) Viability of SH-SY5Y cells incubated with α SN oligomers with or without co-incubation with Koroneiki (0.15 mg/ml).

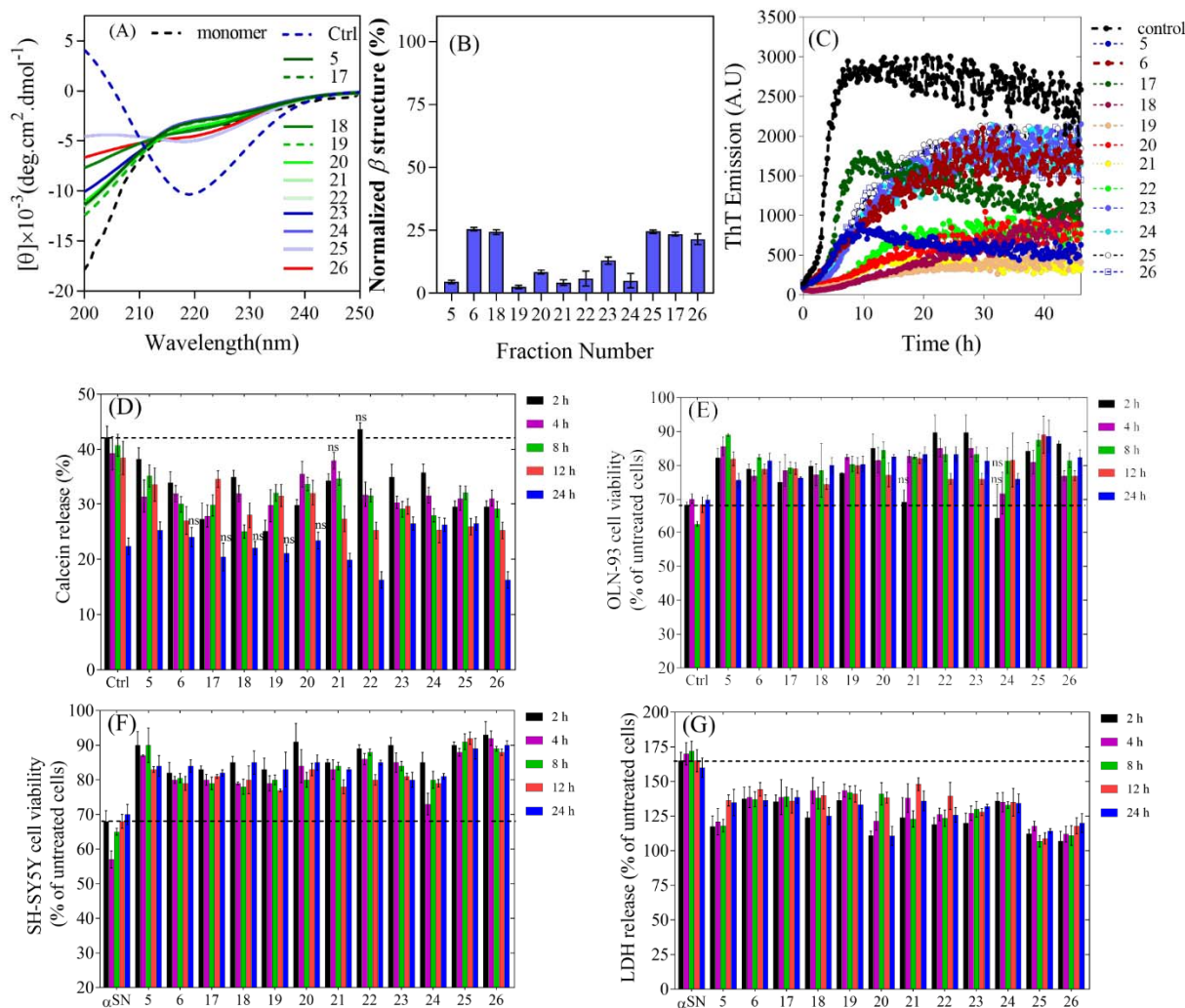


Fig. 6. (A) Far-UV CD spectra of α SN incubated alone (control) and in the presence of 3 mg/ml of Koroneiki extract fractions. (B) Normalized β structure (%) of α SN incubated in the presence of Koroneiki extract fractions. (C) The effect of the Koroneiki extract fractions (1.5 mg/ml) on the seeding of α SN aggregation under shaking conditions. (D) Calcein release from DOPG vesicles after 20 min incubation with α SN aggregates formed alone and in the presence of Koroneiki extract fractions (3 mg/ml) over different times (0-24 h). Viability of (E) OLN-93 and (F) SH-SY5Y cells after 24 h incubation with α SN aggregates formed alone and in the presence of Koroneiki extract fractions (3 mg/ml) over different times (0-24 h). (G) Cytotoxicity of α SN aggregates to SH-SY5Y cells was assayed by LDH-release. LDH signals were normalized to untreated cells. For all assays, values represent means \pm SD and the differences between the groups and α SN control are significant ($P < 0.05$) unless it has "ns" mark.

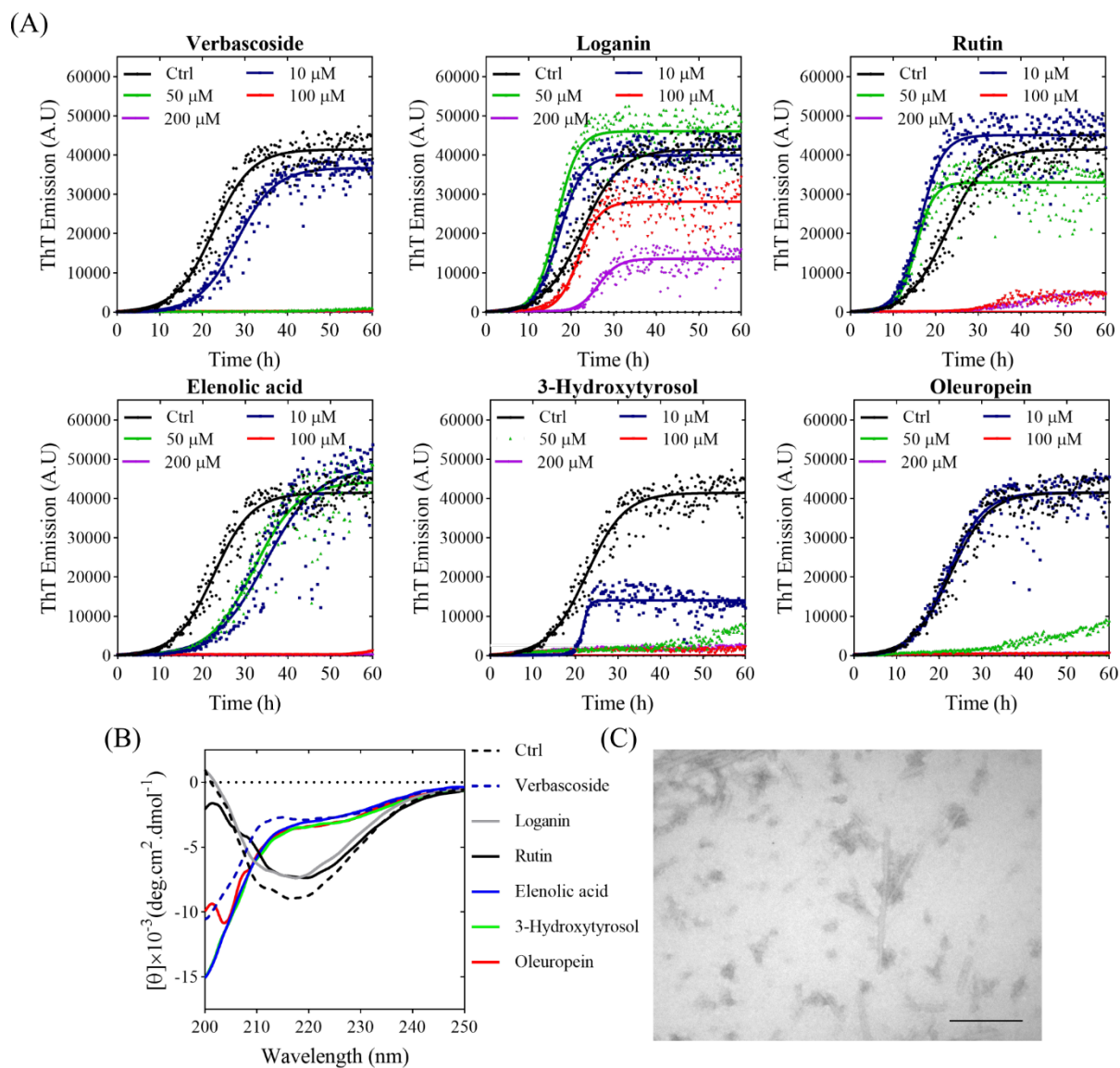


Fig. 7. The effect of Koroneiki compounds on fibrillation of 1 mg/ml α SN. (A) The kinetics of α SN fibrillation in the presence of 0-200 μ M of Koroneiki compounds, monitored by ThT fluorescence. (B) Far-UV CD spectra of α SN incubated alone (Ctrl) and in the presence of 200 μ M of Koroneiki compounds after 24 h. (C) Electron microscopy of α SN after 24 h incubation in the presence of 200 μ M oleuropein. Scale bar: 200 nm.

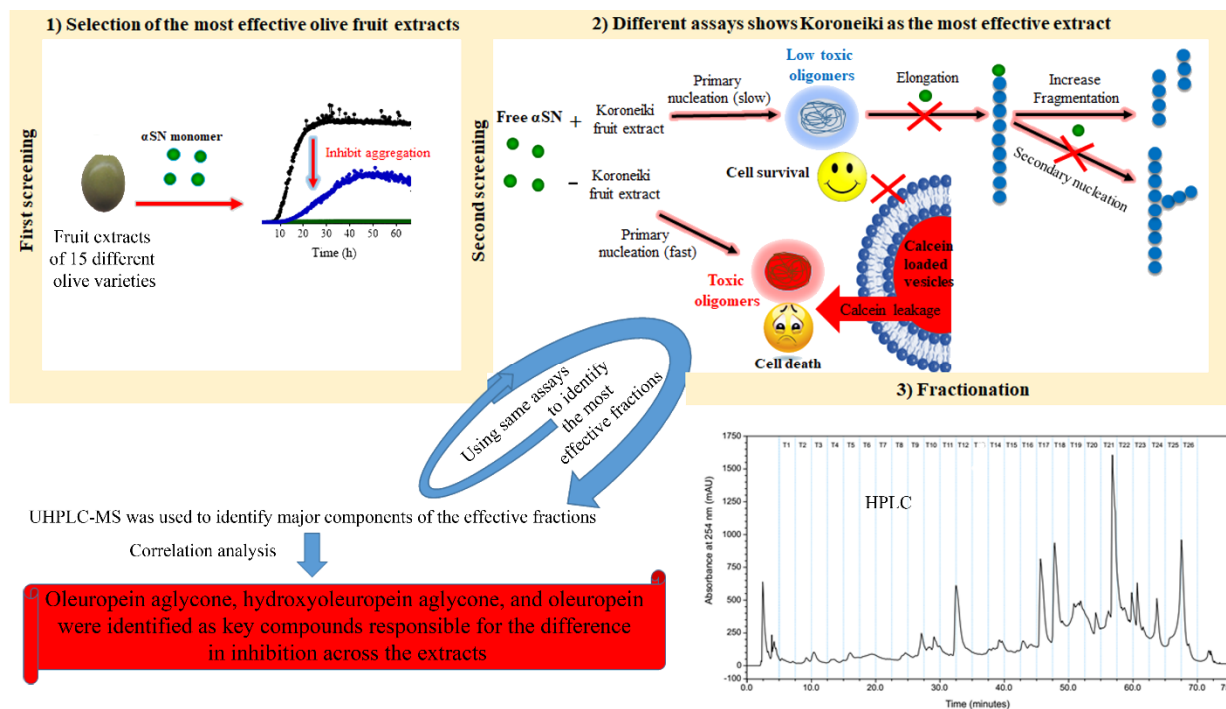


Fig. 8. Schematic representation of screening of different olive varieties. (1) The first screening of fruit extract of 15 different olive varieties on the kinetic analysis of α SN fibrillation. (2) The most effective variety, Koroneiki, combined strong inhibition of α SN fibril nucleation and elongation with strong ability to disaggregate preformed fibrils and prevent formation of toxic α SN oligomers. (3) Koroneiki fruit extract was fractionated and by using the same assay as the ones used in step 2, the most effective fractions were identified. LS-MS analysis was further used to identify the major compounds in the effective fractions. Correlation analysis confirmed oleuropein aglycone, hydroxyoleuropein aglycone, and oleuropein as key compounds responsible for the difference in inhibition across the extracts.

Oleuropein derivatives from olive fruit extracts reduce α -synuclein fibrillation and oligomer toxicity

Hossein Mohammad-Beigi, Farhang Aliakbari, Cagla Sahin, Charlotte Lomax, Ahmed Tawfike, Nicholas P. Schafer, Alireza Amiri-Nowdijeh, Hoda Eskandari, Ian Max Møller, Mehdi Hosseini-Mazinani, Gunna Christiansen, Jane L Ward, Dina Morshedi and Daniel E. Otzen

J. Biol. Chem. published online January 17, 2019

Access the most updated version of this article at doi: [10.1074/jbc.RA118.005723](https://doi.org/10.1074/jbc.RA118.005723)

Alerts:

- [When this article is cited](#)
- [When a correction for this article is posted](#)

[Click here](#) to choose from all of JBC's e-mail alerts

Oleuropein derivatives from olive fruit extracts reduce α -synuclein fibrillation and oligomer toxicity

Hossein Mohammad-Beigi, Farhang Aliakbari, Cagla Sahin, Charlotte Lomax, Ahmed Tawfike, Nicholas P. Schafer, Alireza Amiri-Nowdijeh, Hoda Eskandari, Ian Max Møller, Mehdi Hosseini-Mazinani, Gunna Christiansen, Jane L. Ward, Dina Morshedi, Daniel E. Otzen

Supplementary Figures S1-14 and Tables S1-3

Supplementary Figures

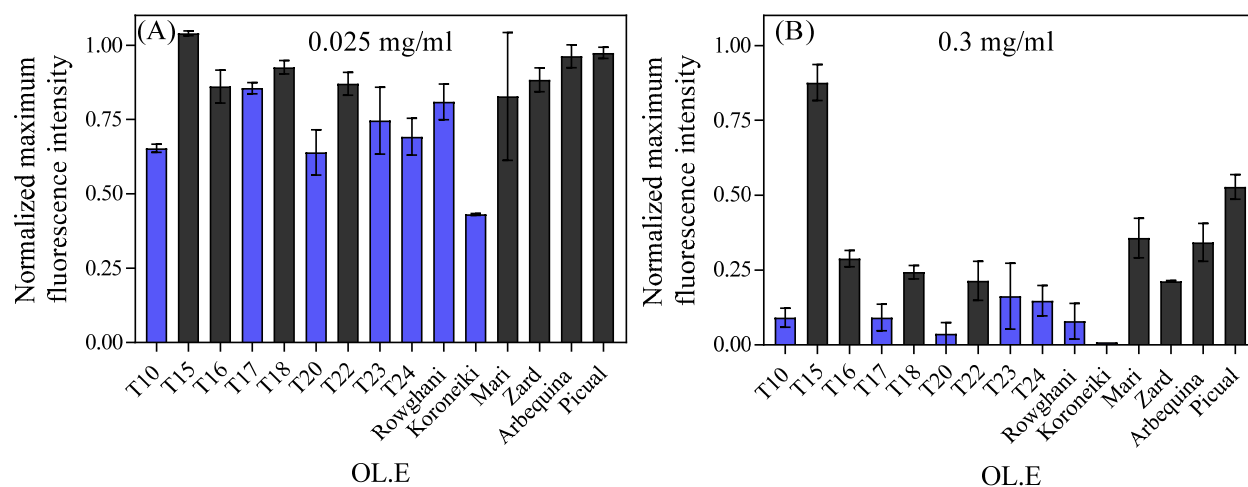


Fig. S1. The effect of different olive fruit extracts on α SN fibrillation. First screening: Selection of the best extracts by the effect of (A) 0.025 mg/ml extract and (B) 0.3 mg/ml extract on the end-point ThT fluorescence level at 1 mg/ml α SN.

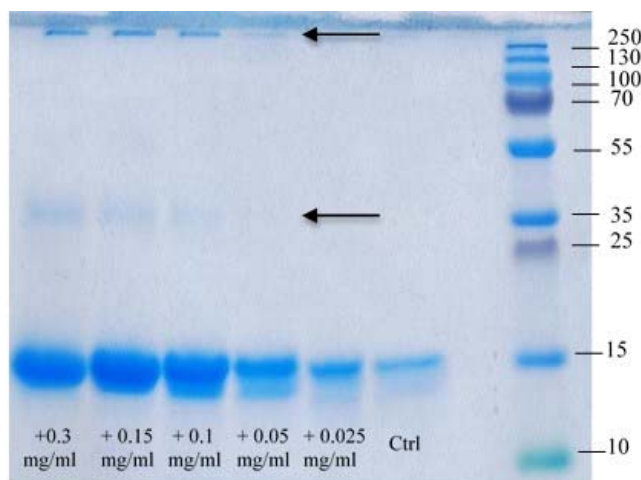
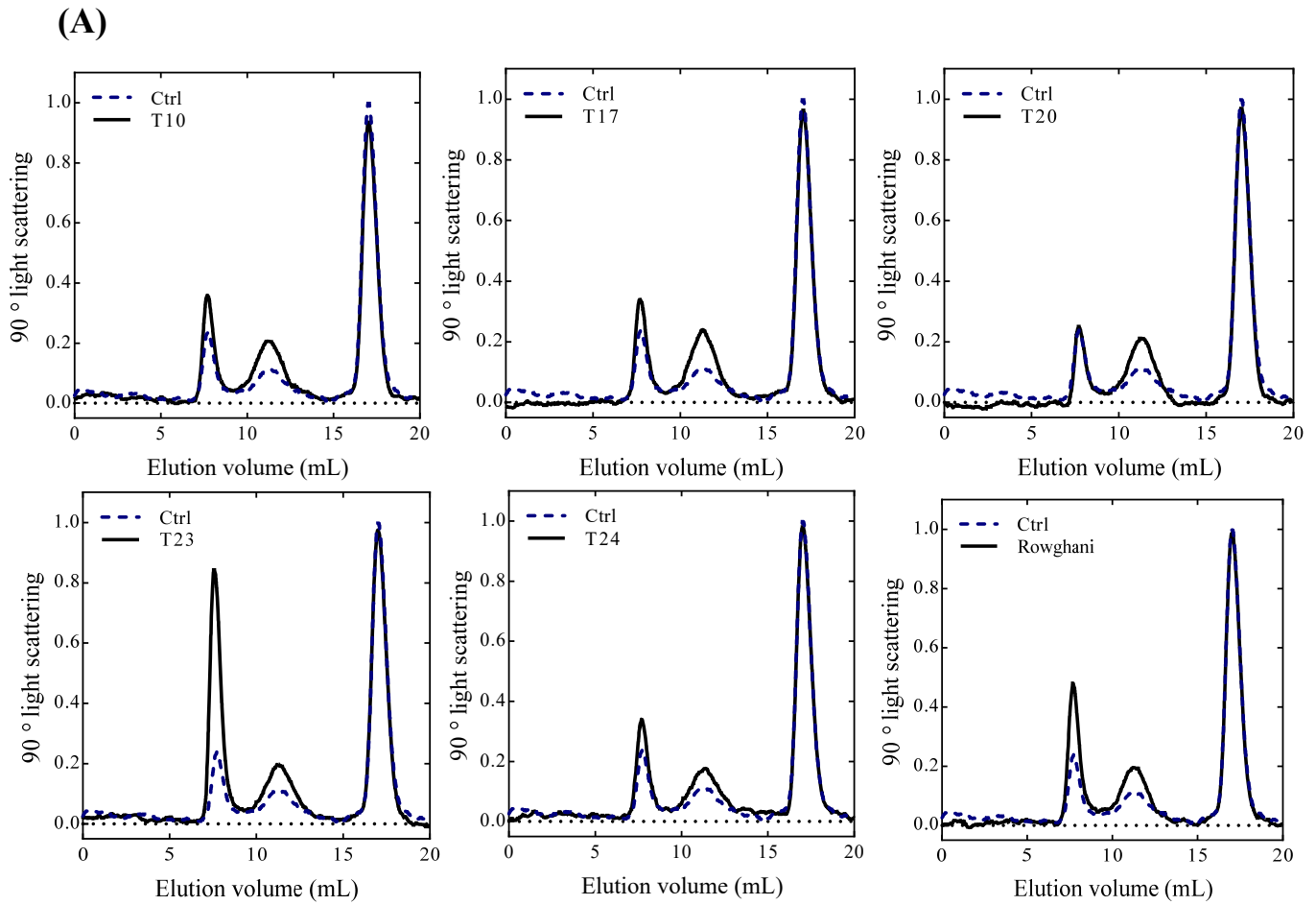


Fig. S2. SDS-PAGE analysis of the supernatants of samples of 1 mg/ml α SN incubated for 24 h in the presence of 0-0.3 mg/ml of of Koroneiki extract. Arrows highlight dimers (\approx 35 kDa) and oligomers ($>$ 250 kDa).



(B)

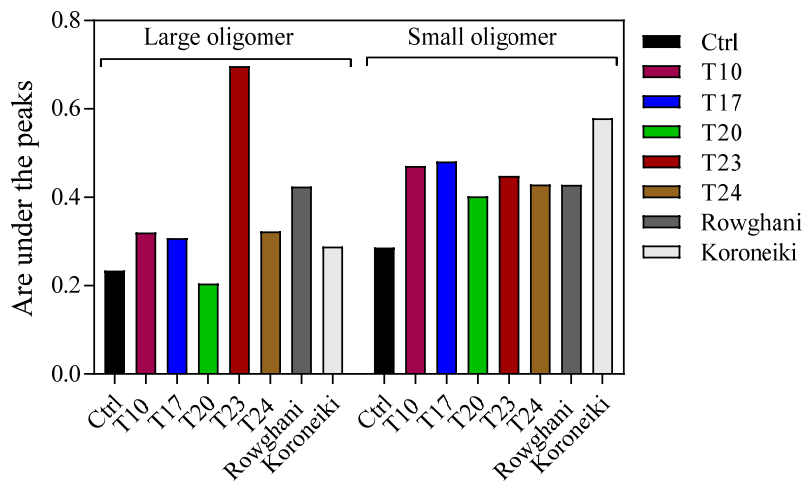


Fig. S3. Oligomerization assay. (A) SEC profile of the supernatants from solutions of 1 mg/ml α SN incubated for 1 h at 37°C in the presence of different extracts. (B) Area under the peaks of small and large oligomers formed in the absence (Ctrl) and presence of 0.15 mg/ml of the best extracts.

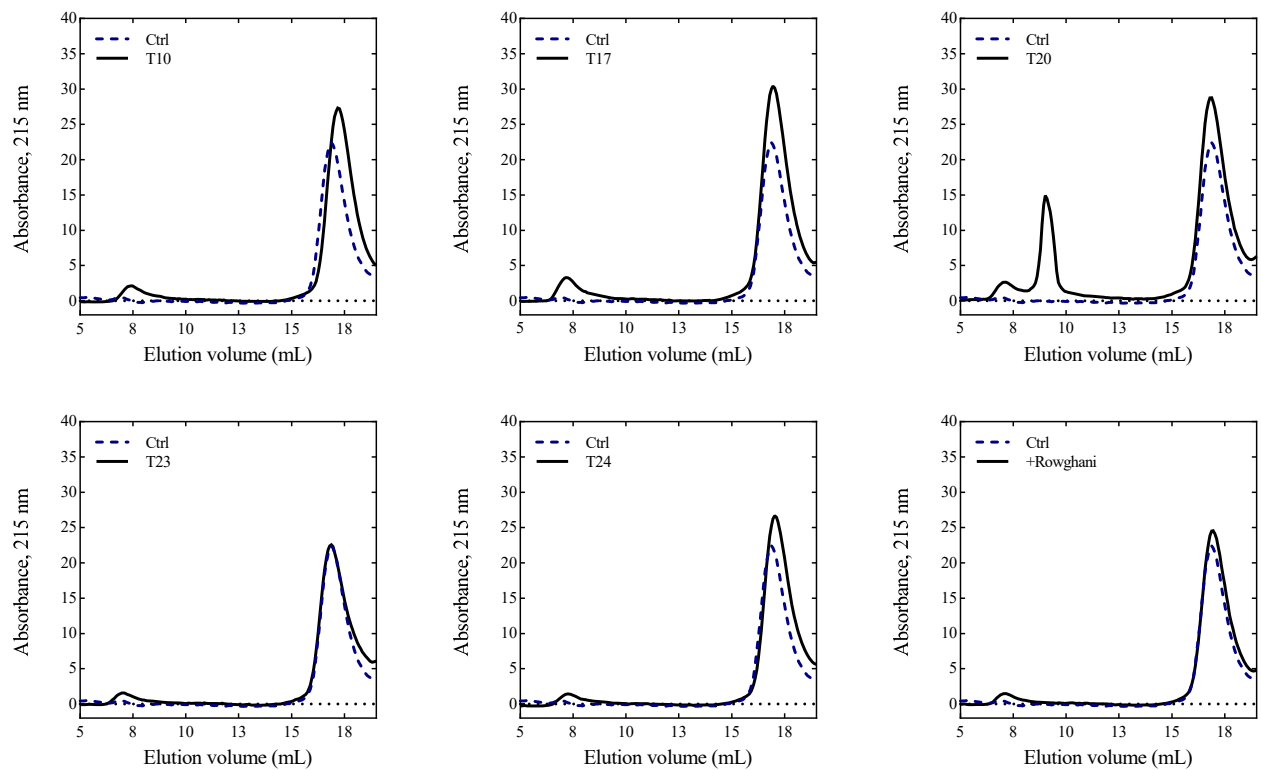


Fig. S4. Disaggregation assay. SEC profile of the supernatants of preformed α SN fibrils incubated at 0.5 mg/ml overnight at 37°C in the absence (Ctrl) and presence of 0.15 mg/ml of the best extracts.

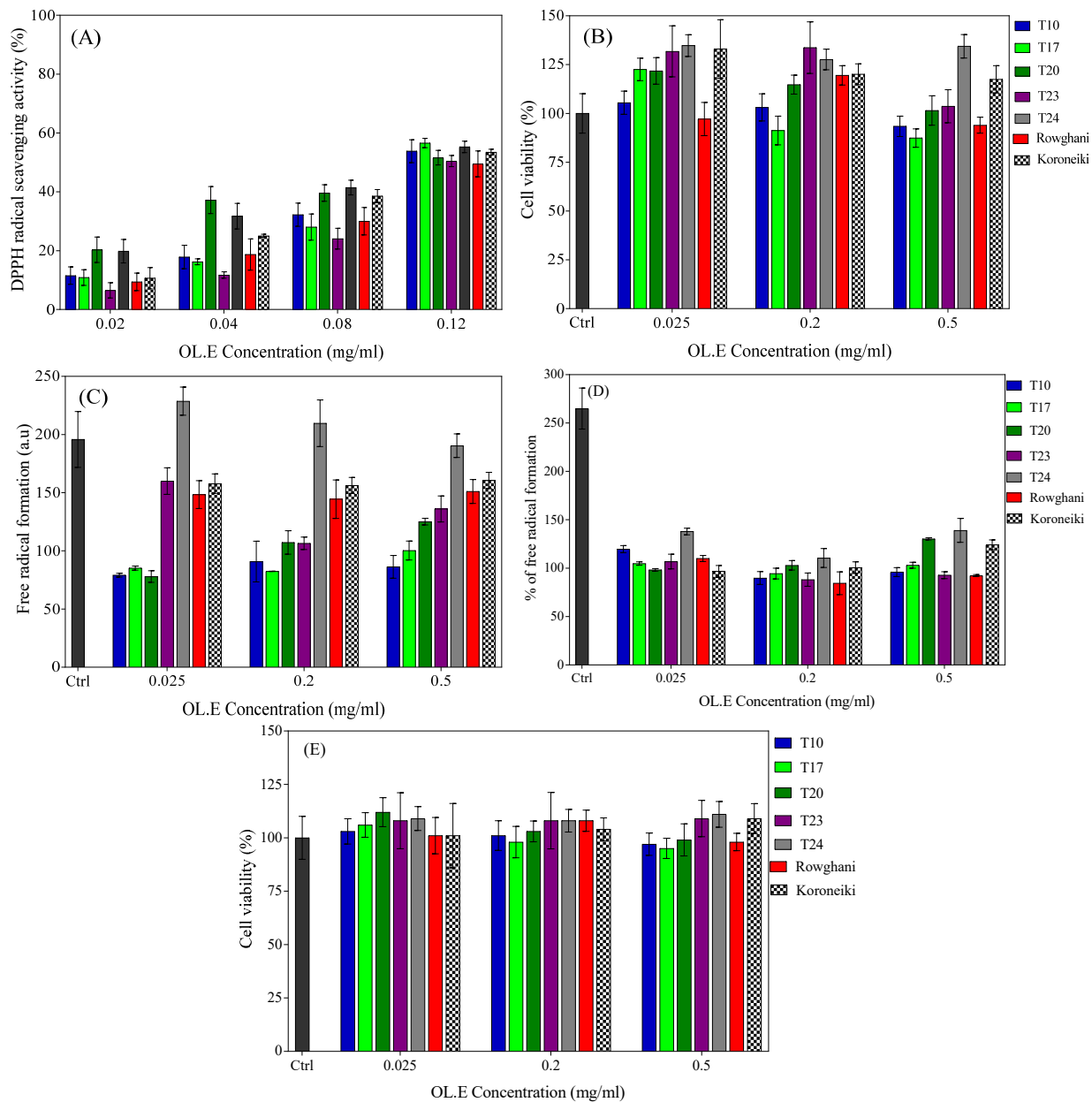


Fig. S5. Antioxidant activity and toxicity of the olive extracts. (A) Antioxidant activity of different olive fruit extracts at different concentrations (0.02, 0.04, 0.08, 0.12 mg/ml) measured by DPPH assay. (B) Viability of OLN-93 cells after 24 h incubation with the best olive extracts at different concentrations (0.025, 0.2, 0.5 mg/ml). (C) Oxidative stress in OLN-93 cells treated with olive extracts at different concentrations determined by DCFH-DA assay. (D) Free radical scavenging ability of the olive extracts measured in OLN-93 cells treated with 100 μ M H₂O₂. (E) Viability of SH-SY5Y cells after 24 h incubation with 0-0.5 mg/ml of the best olive extracts.

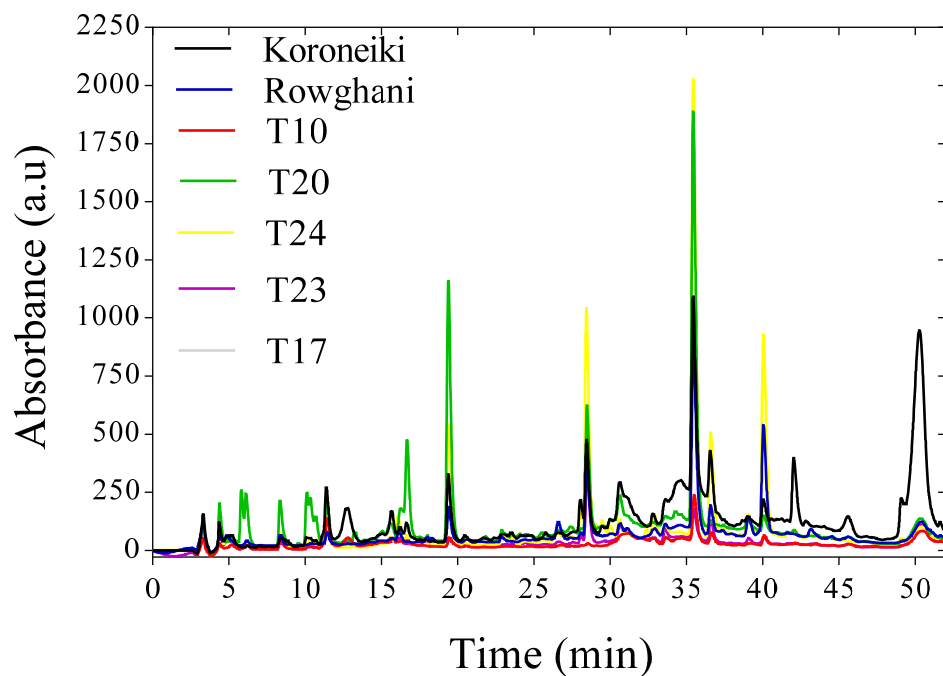


Fig. S6. HPLC chromatograms of the 7 most efficient anti-aggregative olive extracts, recorded at 230 nm.

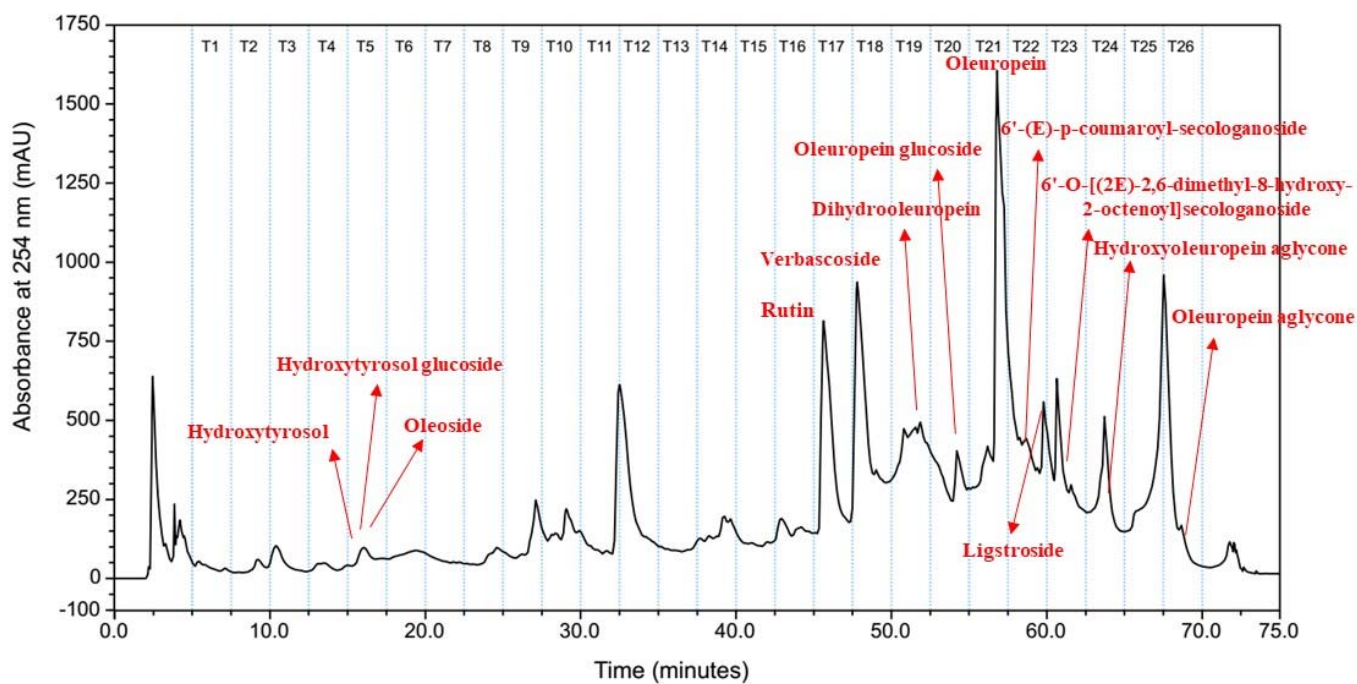


Fig. S7. Chromatogram of Koroneiki extract using HPLC. Fractions T1-26 are indicated. The different were identified by HPLC-MS.

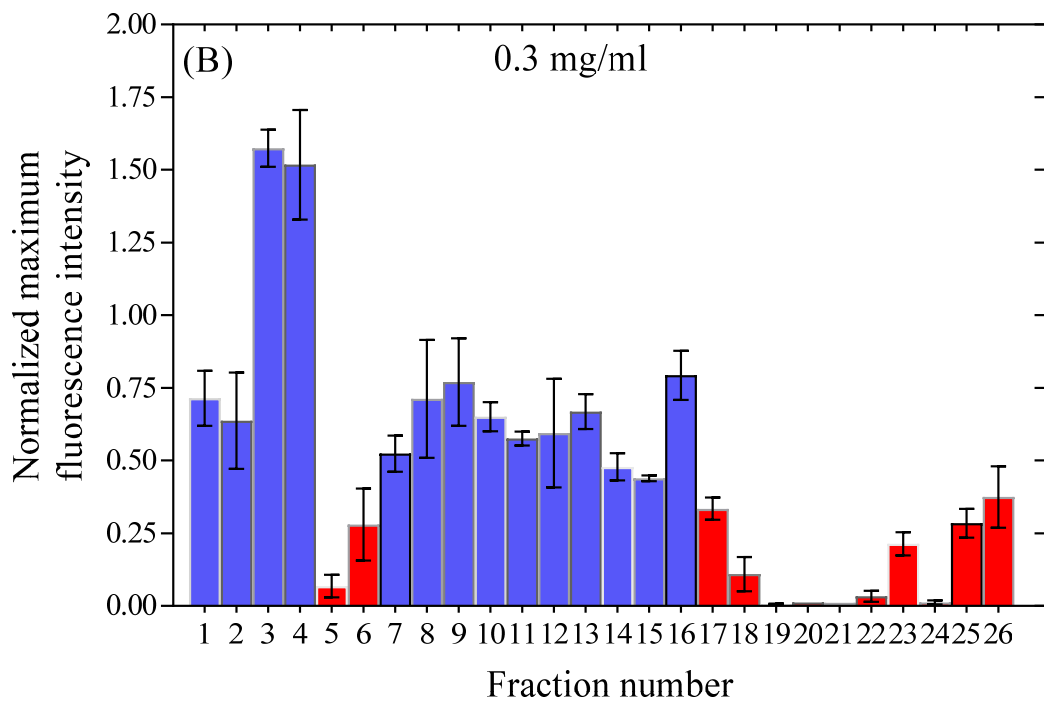
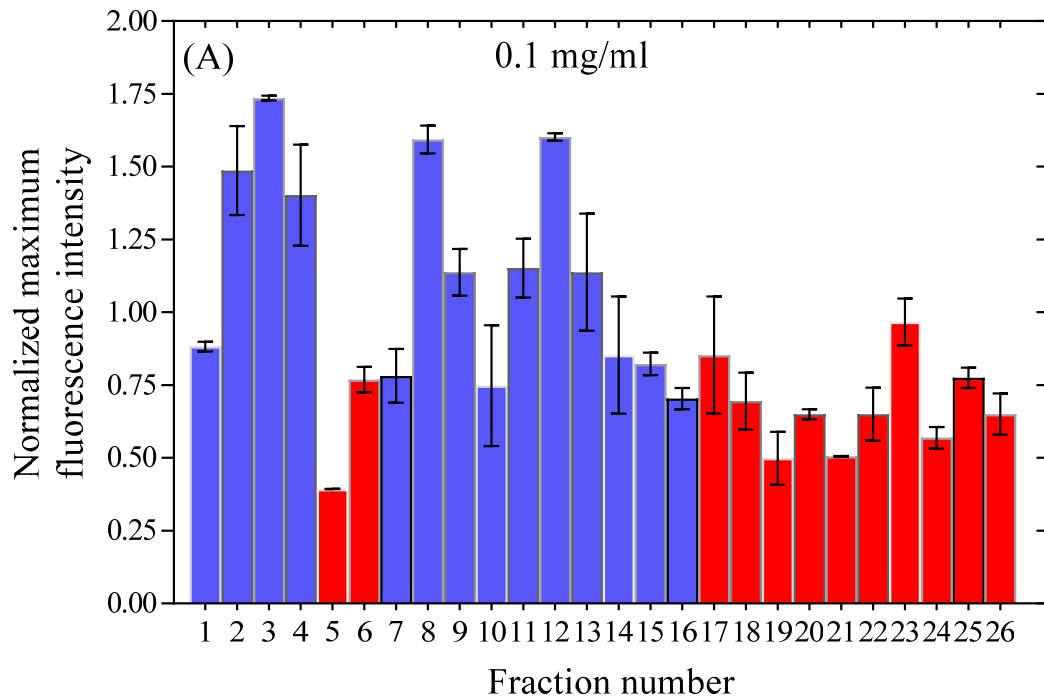


Fig. S8. The effect of (A) 1 mg/ml and (B) 3 mg/ml of the Koroneiki extract fractions on fibrillation of 1 mg/ml α SN. Maximum ThT fluorescence intensity normalized to control (absence of extract).

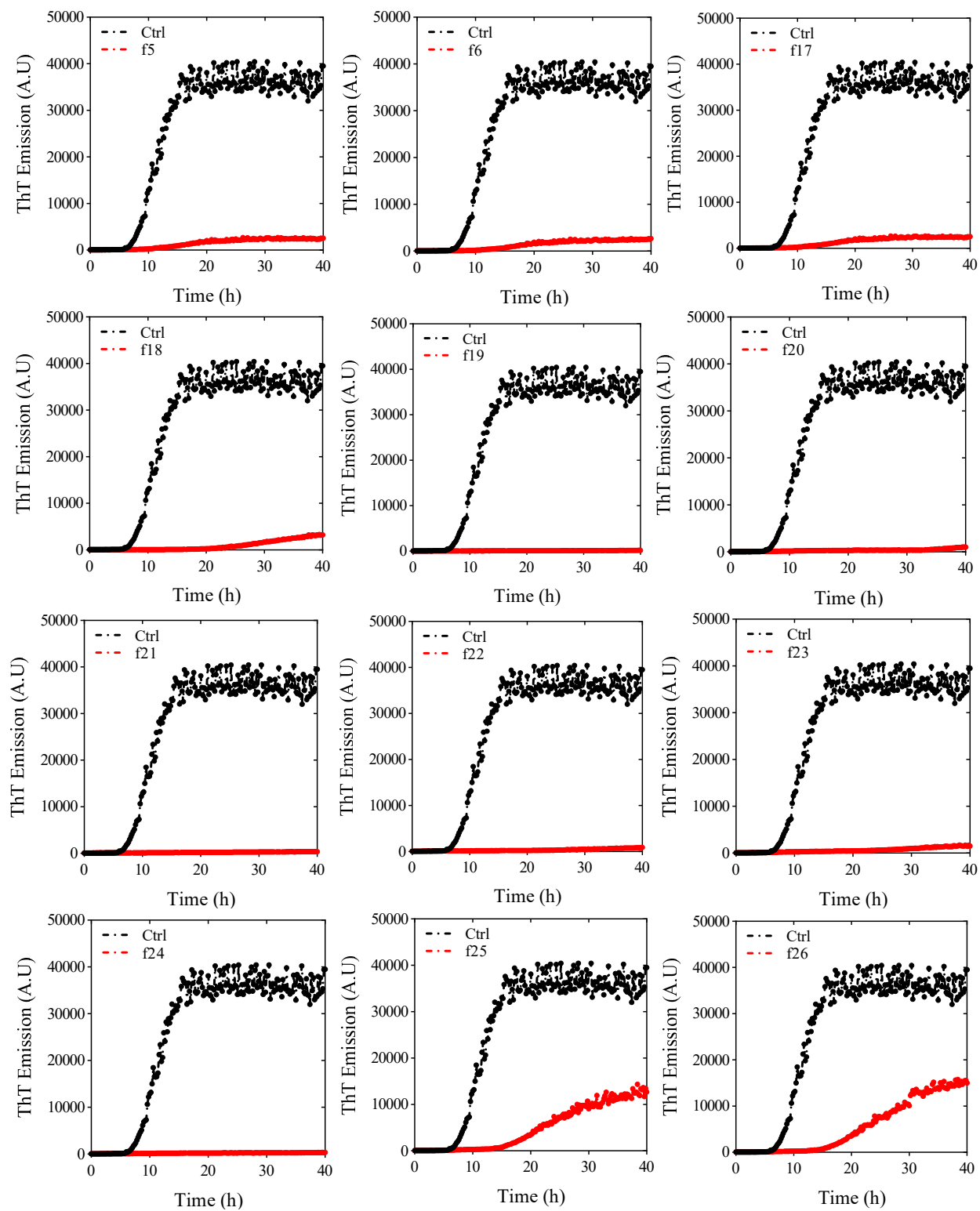


Fig. S9. The effect of Koroneiki extract fractions (3 mg/ml) on the kinetics of fibrillation of 1 mg/ml α SN monitored by ThT fluorescence.

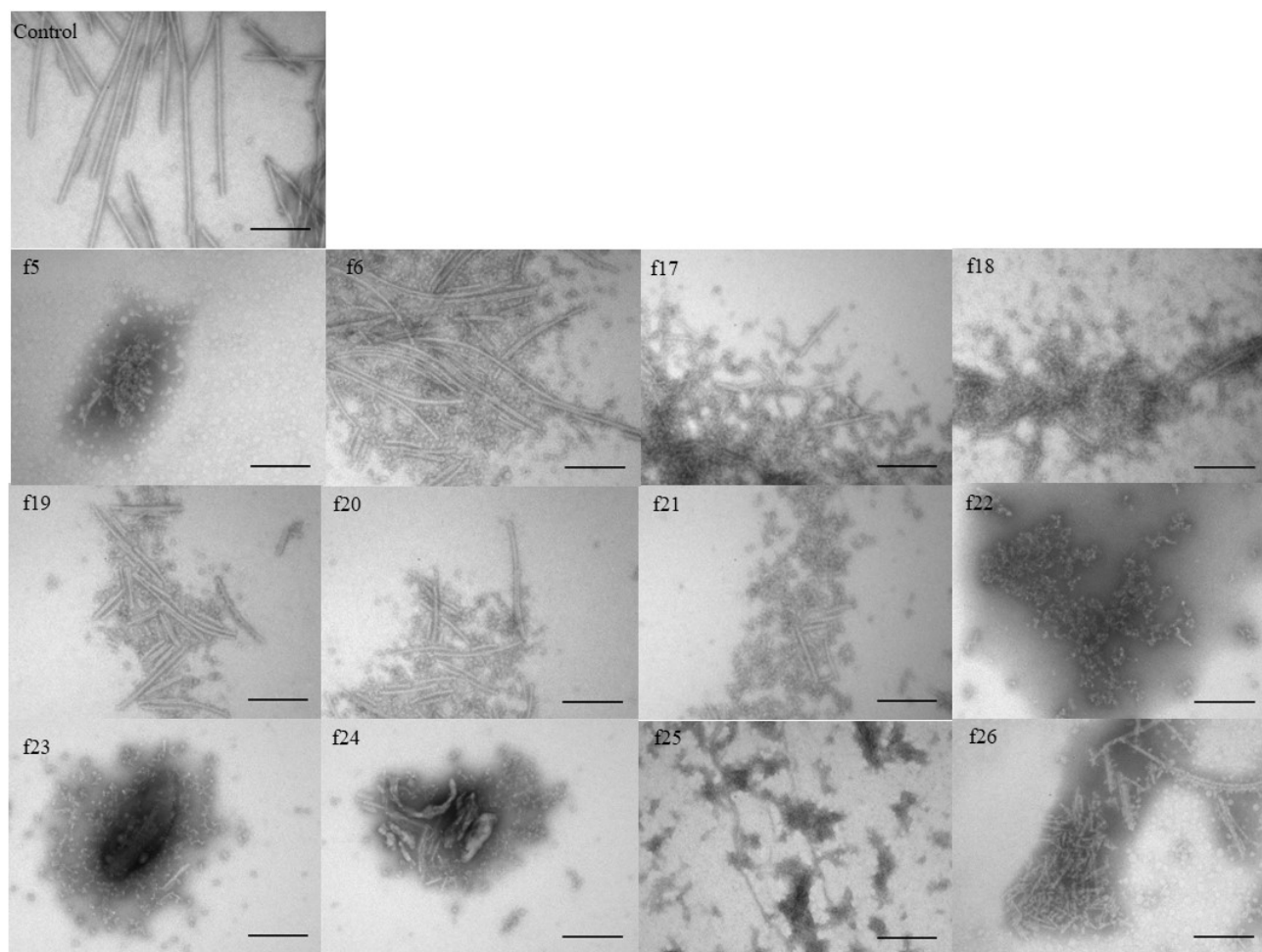
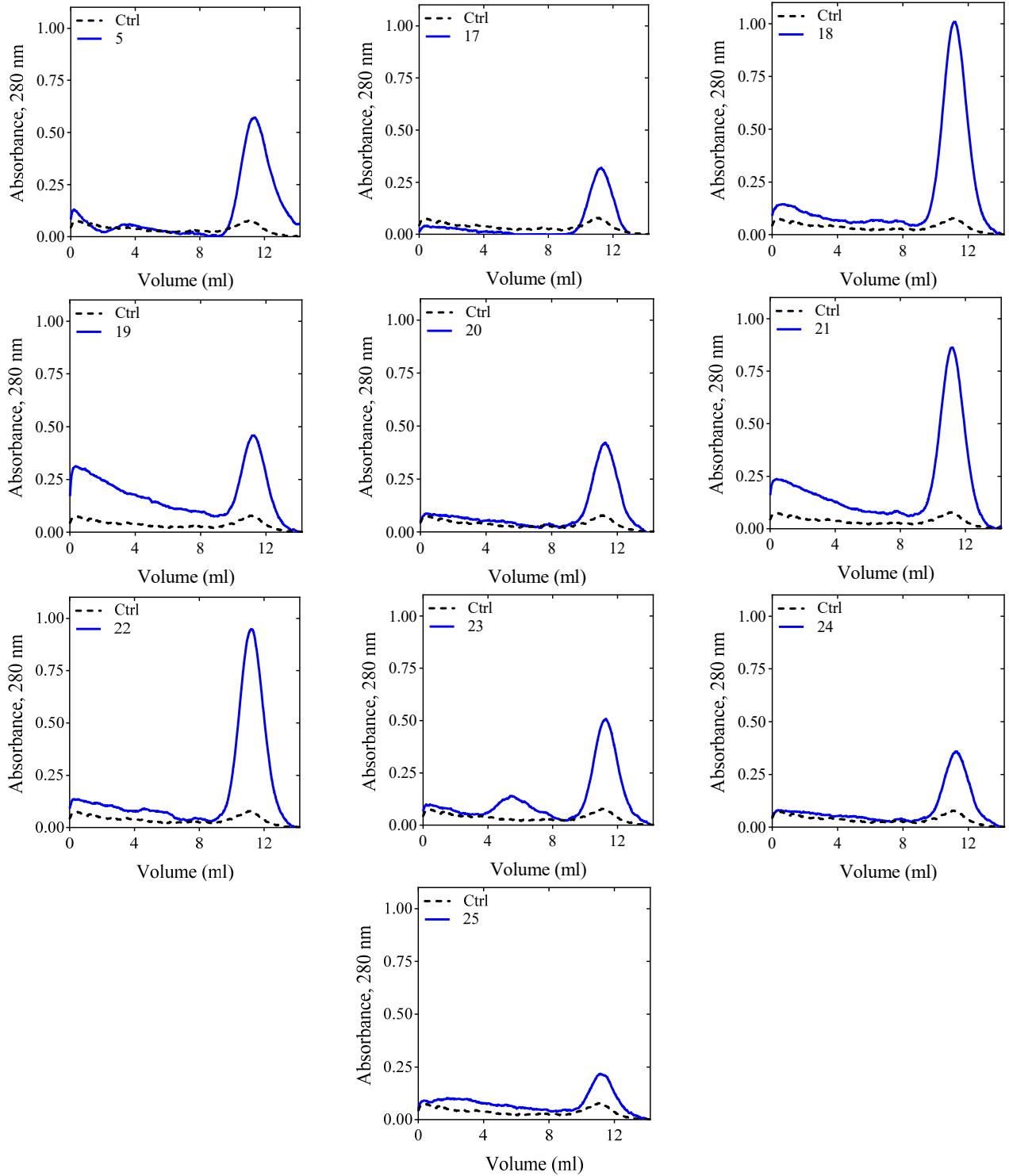


Fig. S10. TEM images of 1 mg/ml α SN incubated alone (control) and in the presence of 3 mg/ml of Koroneiki extract fractions.

(A)



(B)

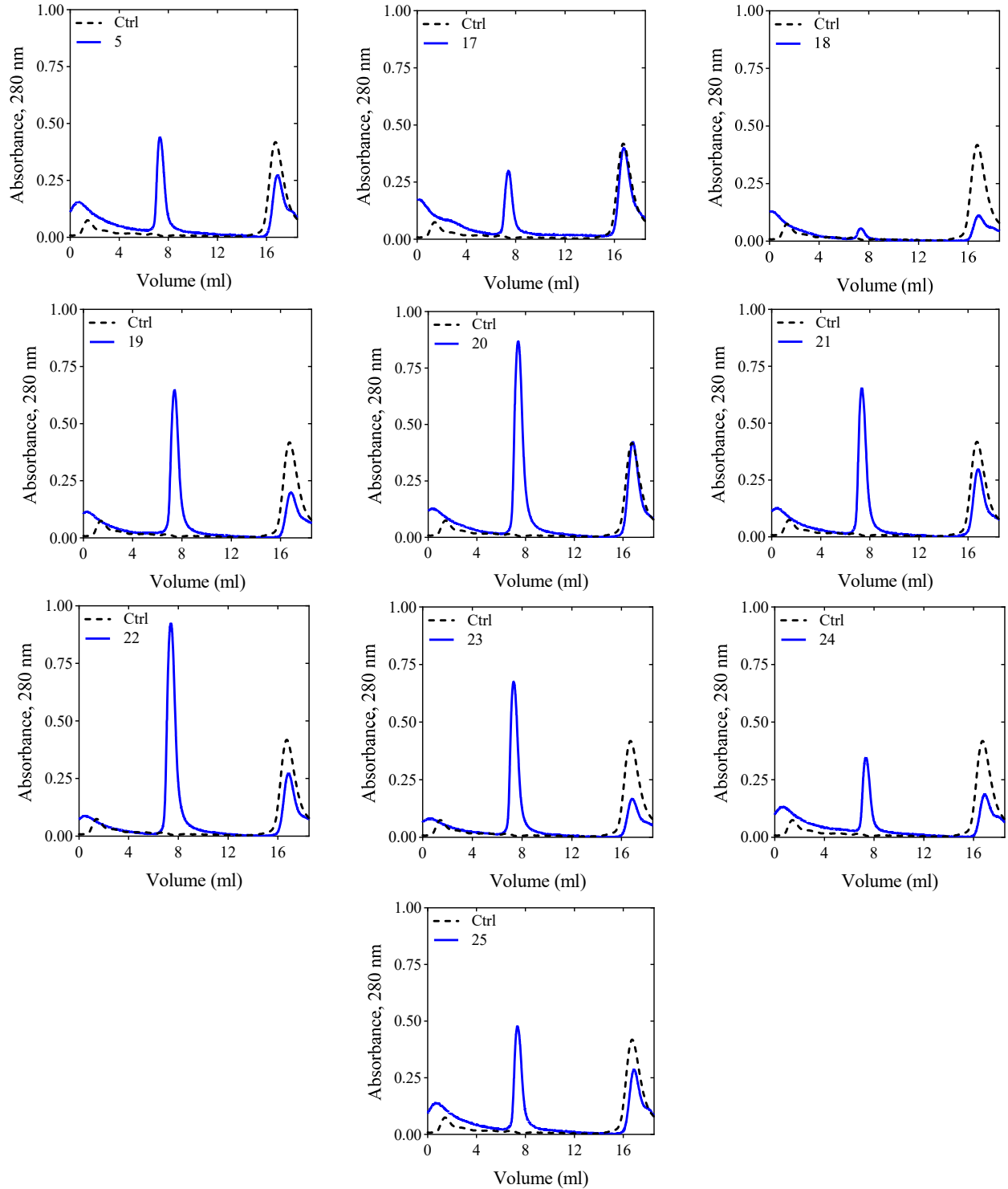


Fig. S11. SEC profiles of the supernatants of (A) samples of 1 mg/ml α SN incubated for 1 h at 37°C in an oligomerization assay and (B) 0.5 mg/ml preformed α SN fibrils preincubated overnight at 37°C with and without 3 mg/ml of Koroneiki extract fractions in a disaggregation assay.

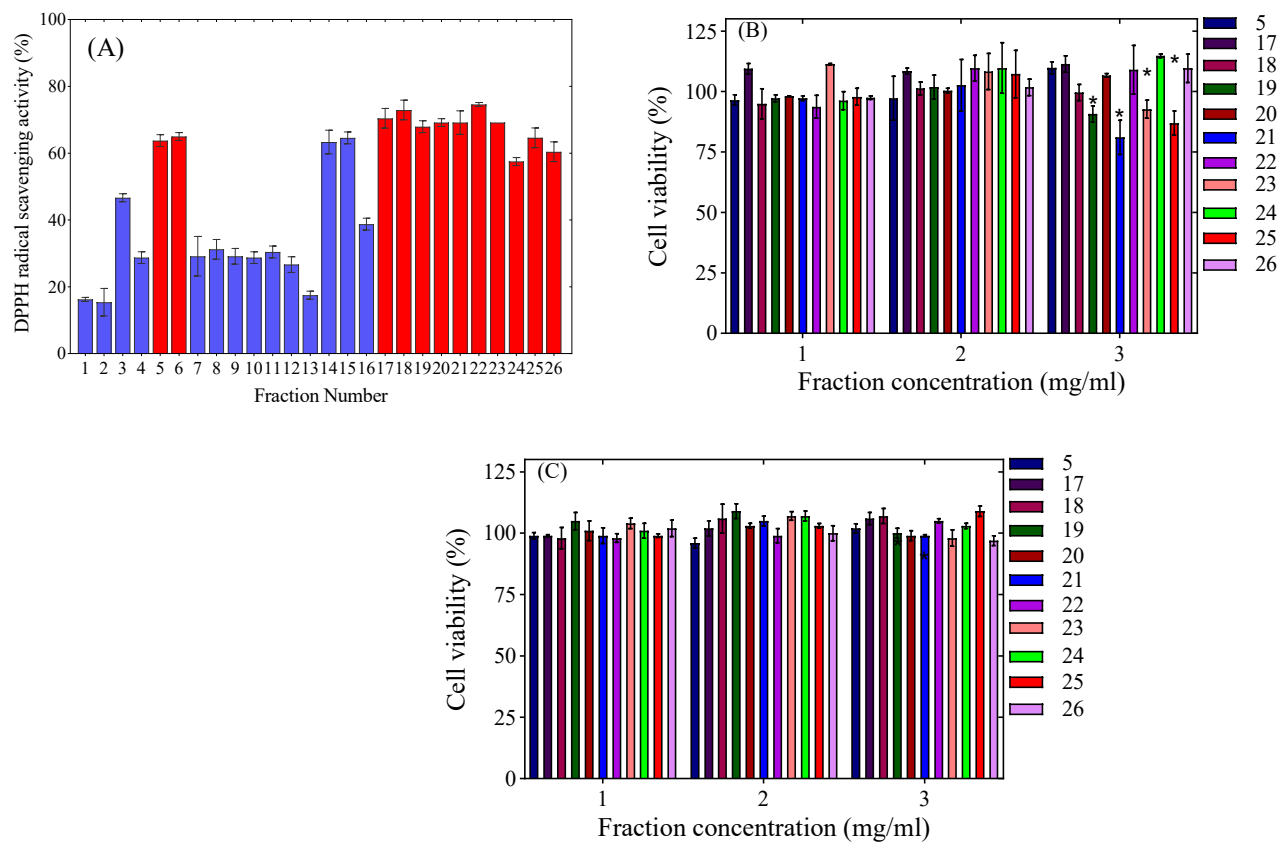


Fig. S12. (A) Antioxidant activity of Koroneiki extract fractions (3 mg/ml) measured by DPPH assay. Viability of (B) OLN-93 and (C) SH-SY5Y cells after 24 h incubation with 1-3 mg/ml Koroneiki extract fractions.

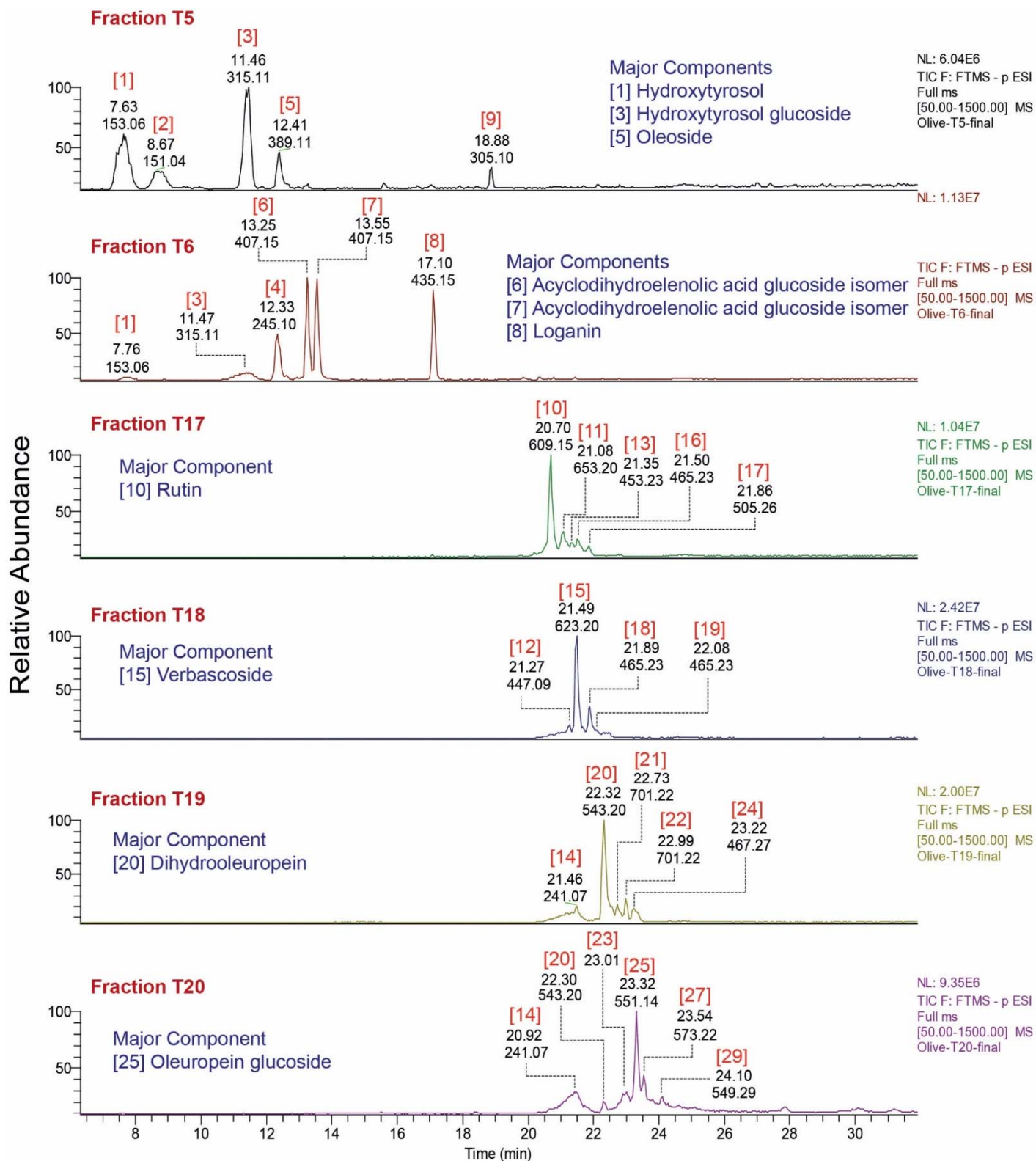


Fig. S13. Total ion chromatograms of Koroneiki fractions

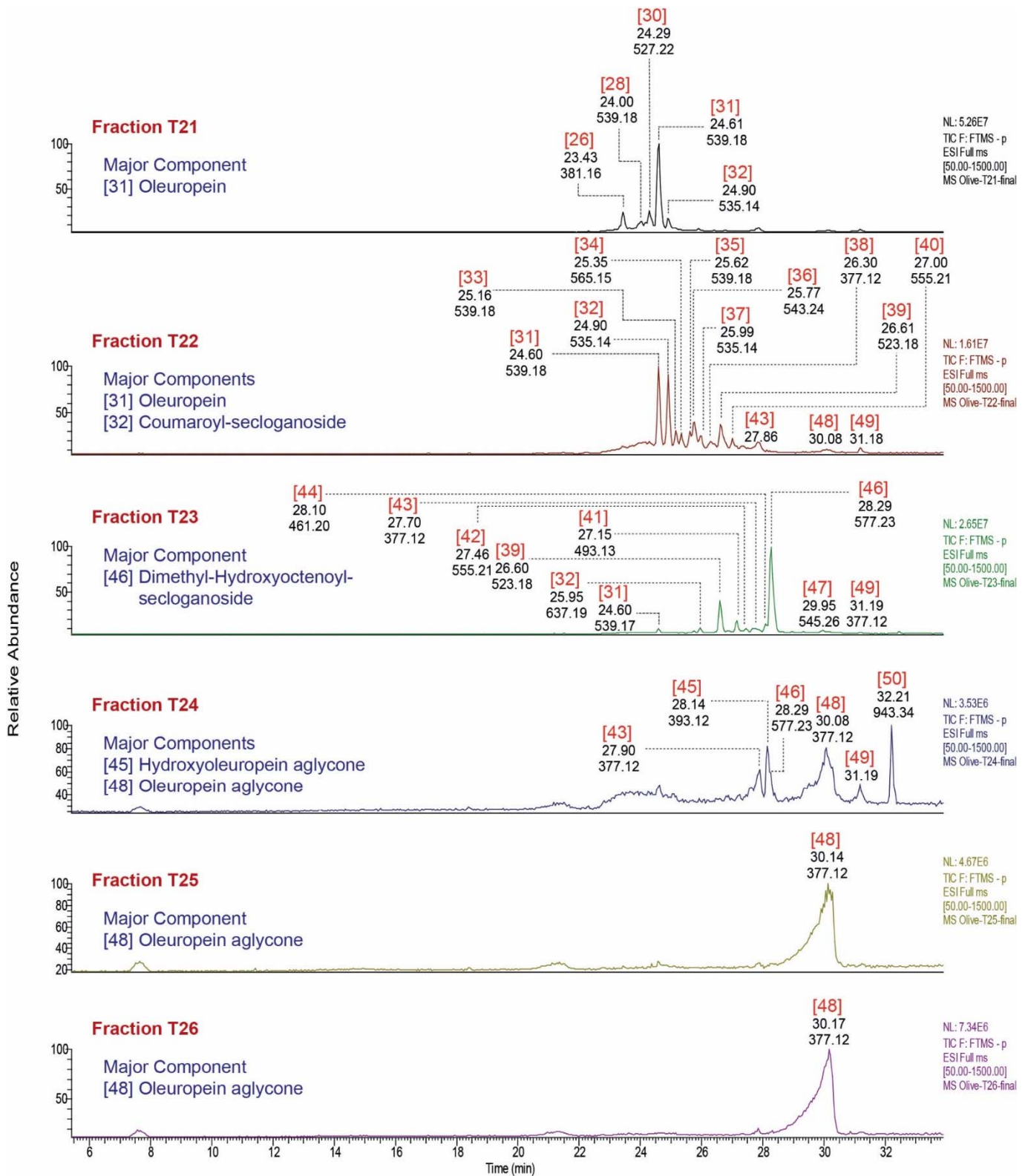


Fig. S13 (cont'd). Total ion chromatograms of Koroneiki fractions.

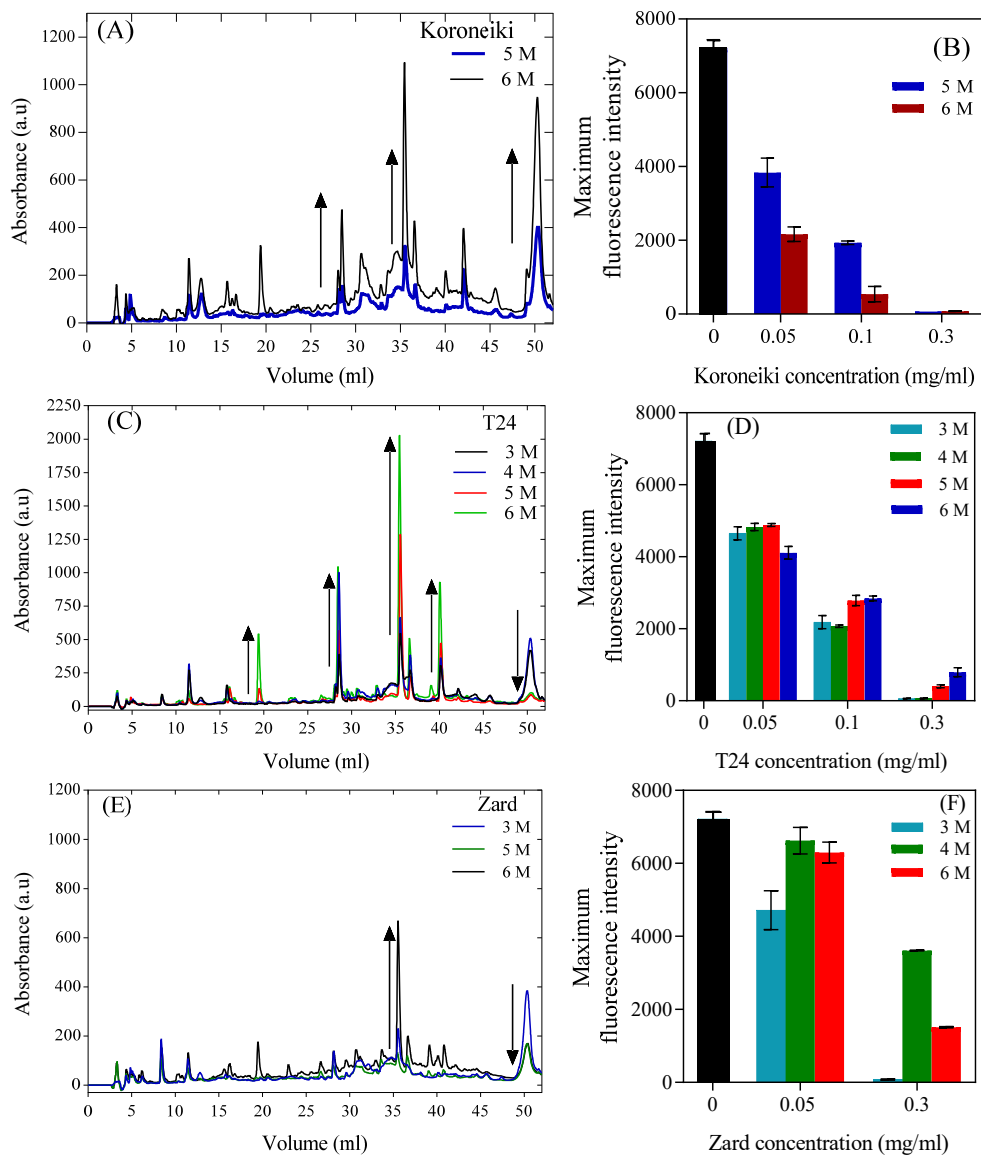


Fig. S14. Change in the level of compounds in the extracts of fruits picked at different maturation time (3, 4, 5, and 6 months after flowering) and their inhibitory effect on α SN fibrillation. HPLC chromatogram of the extracts (A, C, and E) and their effect on the maximum ThT fluorescence intensity (B, D, and F)

Table S1. Olive cultivars used in this study.

Nr	Olive Cultivar	Abbreviation	Origin	Nr	Olive Cultivar	Abbreviation	Origin
1	Koroneiki	-	Greece	9	Chenaran	T16	Iran
2	Arbequina	-	Spain	10	Khoshe	T17	Iran
3	Picual	-	Spain	11	Parseh	T18	Iran
4	Mari	-	Iran	12	Majnon	T20	Iran
5	Rowghani	-	Iran	13	Tak	T22	Iran
6	Zard	-	Iran	14	Zarin	T23	Iran
7	Yaghout	T10	Iran	15	Arghavan	T24	Iran
8	Gorgan	T15	Iran				

Table S2. LC-MS data of fractions f5, 6, and 17-26 of Koroneiki extract obtained from HPLC separation

Peak	Retention time (min)	m/z	Predicted ion formula	Delta (ppm)	MS-MS	λ_{max}	Identity or Compound class	How identified	Previously observed in <i>Olea</i> species? (reference)
1	7.63	153.0556	[C ₈ H ₉ O ₃] ⁻	0.94	123 (C ₇ H ₇ O ₂)	281	Hydroxytyrosol	authentic standard	Yes (1)
2	8.67	151.0401	[C ₈ H ₇ O ₃] ⁻	1.49	-	280	4-Hydroxyphenylacetate	Accurate mass.	Yes (1)
3	11.46	315.1086	[C ₁₄ H ₁₉ O ₈] ⁻	1.29	153 (C ₈ H ₉ O ₃)	278	Hydroxytyrosol glucoside	MSMS and literature data ^a	Yes (1)
4	12.33	245.1034	[C ₁₁ H ₁₇ O ₆] ⁻	1.39	-	-	Unknown	-	-
5	12.41	389.1090	[C ₁₆ H ₂₁ O ₁₁] ⁻	1.11	227 (C ₁₀ H ₁₁ O ₆), 183 (C ₉ H ₁₁ O ₄), 165 (C ₉ H ₉ O ₃), 121 (C ₈ H ₉ O), 89 (C ₃ H ₅ O ₃)		Oleoside	RT, MS, MSMS and literature data ^b	Yes (2)
6	13.25	407.1560	[C ₁₇ H ₂₇ O ₁₁] ⁻	1.21	389 (C ₁₇ H ₂₅ O ₁₀), 377 (C ₁₆ H ₂₅ O ₁₀), 357 (C ₁₆ H ₂₁ O ₉), 313 (C ₁₅ H ₂₁ O ₇), 183 (C ₁₀ H ₁₅ O ₃), 151 (C ₉ H ₁₁ O ₂), 113 (C ₅ H ₅ O ₃), 101 (C ₄ H ₅ O ₃), 89 (C ₃ H ₅ O ₃)		Glucosyl acyclodihydroelenolic acid isomer I	Putative from MSMS.	Yes (3)
7	13.55	407.1560	[C ₁₇ H ₂₇ O ₁₁] ⁻	1.24	389 (C ₁₇ H ₂₅ O ₁₀), 377 (C ₁₆ H ₂₅ O ₁₀), 357 (C ₁₆ H ₂₁ O ₉), 313 (C ₁₅ H ₂₁ O ₇), 183 (C ₁₀ H ₁₅ O ₃), 151 (C ₉ H ₁₁ O ₂), 113 (C ₅ H ₅ O ₃), 101 (C ₄ H ₅ O ₃), 89 (C ₃ H ₅ O ₃)		Glucosyl acyclodihydroelenolic acid.isomer II	Putative from MSMS. Identical to Peak 6	Yes (3)
8	17.10	435.1506	[C ₁₈ H ₂₇ O ₁₂] ⁻	0.877	357 (C ₁₆ H ₂₁ O ₉), 313 (C ₁₅ H ₂₁ O ₇), 183 (C ₁₀ H ₁₅ O ₃), 169 (C ₉ H ₁₃ O ₃), 151 (C ₉ H ₁₁ O ₂), 113 (C ₅ H ₅ O ₃), 101	219	Formate adduct of Loganin(C ₁₇ H ₂₅ O ₁₀)	RT, MS, MSMS and literature data ^b	Yes (2)

					(C ₄ H ₅ O ₃), 89 (C ₃ H ₅ O ₃)				
9	18.88	305.1038	[C ₁₆ H ₁₇ O ₆] ⁻	1.82	153 (C ₈ H ₉ O ₃), 151 (C ₈ H ₇ O ₃), 123 (C ₇ H ₇ O ₂)	217	Conjugate of hydroxytyrosol and hydroxyphenyl acetate (ie 4-(hydroxyphenyl)ethyl 2-(4-hydroxyphenyl)acetate) OR conjugate of Vanillin and hydroxy tyrosol	Putative based on MS/MSMS fragmentati on	-
10	20.70	609.1514	[C ₂₇ H ₂₉ O ₁₆] ⁻	1.17	300 (C ₁₅ H ₈ O ₇)	253, 354	Rutin	Authentic standard	Yes (2)
11	21.08	653.2030	[C ₃₀ H ₃₇ O ₁₆] ⁻	1.30	621 (C ₂₉ H ₃₃ O ₁₅), 459 (C ₂₀ H ₂₇ O ₁₂), 179 (C ₉ H ₇ O ₄), 161 (C ₉ H ₅ O ₃), 151 (C ₈ H ₇ O ₃)		Methoxyverbascoside	RT, MS, MSMS and literature data ^b	Yes (2)
12	21.27	447.0934	[C ₂₁ H ₁₉ O ₁₁] ⁻	1.18	285 (C ₁₅ H ₉ O ₆)	346	Luteolin-7-glucoside	Authentic standard	Yes (2)
13	21.35	453.2337	[C ₂₀ H ₃₇ O ₁₁] ⁻	0.63	321 (C ₁₅ H ₂₉ O ₇), 233 (C ₉ H ₁₃ O ₇), 191 (C ₇ H ₁₁ O ₆), 161 (C ₆ H ₉ O ₅), 113 (C ₅ H ₅ O ₃), 101 (C ₄ H ₅ O ₃)	218	Unknown	-	-
14	21.46	241.0719	[C ₁₁ H ₁₃ O ₆] ⁻	0.169	139 (C ₆ H ₃ O ₄)	219.,328	Unknown	-	
15	21.49	623.2022	[C ₂₂ H ₃₉ O ₂₀] ⁻	-0.71	461 (C ₁₆ H ₂₉ O ₁₅), 179 (C ₉ H ₇ O ₄), 161 (C ₉ H ₅ O ₃)	330	Verbascoside	RT, MS, MSMS and literature data ^a	Yes (1)
16	21.50	505.2626	[C ₂₄ H ₄₁ O ₁₁] ⁻		251 (C ₉ H ₁₅ O ₈), 191 (C ₇ H ₁₁ O ₆), 149 (C ₅ H ₉ O ₅), 131 (C ₅ H ₇ O ₄), 101 (C ₄ H ₅ O ₃), 89 (C ₃ H ₅ O ₃)		Unknown diglycoside	-	-
17	21.86	505.2625	[C ₂₄ H ₄₁ O ₁₁] ⁻		373 (C ₁₉ H ₃₃ O ₇), 233 (C ₉ H ₁₃ O ₇), 161 (C ₆ H ₉ O ₅), 89 (C ₃ H ₅ O ₃)		Unknown diglycoside	-	-
18	21.89	465.2323	n.d.		333 (C ₁₆ H ₂₉ O ₇), 233 (C ₉ H ₁₃ O ₇), 161 (C ₆ H ₉ O ₅), 113 (C ₅ H ₅ O ₃), 101	218	Unknown		-

					(C ₄ H ₅ O ₃), 89 (C ₃ H ₅ O ₃)				
19	22.08	465.2332	n.d.		333 (C ₁₆ H ₂₉ O ₇), 233 (C ₉ H ₁₃ O ₇), 161 (C ₆ H ₉ O ₅), 113 (C ₅ H ₅ O ₃), 101 (C ₄ H ₅ O ₃), 89 (C ₃ H ₅ O ₃)	218	Unknown, isomer of 18	-	-
20	22.32	543.2047	[C ₂₅ H ₃₅ O ₁₃] ⁻	-2.55	377 (C ₁₆ H ₂₅ O ₁₀), 357 (C ₁₆ H ₂₁ O ₉), 313 (C ₁₅ H ₂₁ O ₇), 197 (C ₁₀ H ₁₃ O ₄), 101 (C ₄ H ₅ O ₃)		Dihydrooleuropein	RT, MS, MSMS. And ref ^d	Yes (4)
		623.2041	[C ₂₂ H ₃₉ O ₂₀] ⁻	1.21	461 (C ₁₆ H ₂₉ O ₁₅), 179 (C ₉ H ₇ O ₄), 161 (C ₉ H ₅ O ₃)		Verbascoside isomer		Yes (2)
21	22.73	701.2235	[C ₃₁ H ₄₁ O ₁₈] ⁻	-5.92	377 (C ₁₉ H ₂₁ O ₈), 307 (C ₁₅ H ₁₅ O ₇), 275 (C ₁₅ H ₁₅ O ₅), 221 (C ₈ H ₁₃ O ₇), 179 (C ₆ H ₁₁ O ₆), 149 (C ₈ H ₅ O ₃), 101 (C ₄ H ₅ O ₃)	219	Oleuropein glycoside isomer	RT, MS, MSMS. And ref ^b	Yes (2)
22	22.99	701.2213	[C ₃₁ H ₄₁ O ₁₈] ⁻	-7.44	377 (C ₁₉ H ₂₁ O ₈), 307 (C ₁₅ H ₁₅ O ₇), 275 (C ₁₅ H ₁₅ O ₅), 221 (C ₈ H ₁₃ O ₇), 179 (C ₆ H ₁₁ O ₆), 149 (C ₈ H ₅ O ₃), 101 (C ₄ H ₅ O ₃)	219	Oleuropein glycoside isomer	RT, MS, MSMS. And ref ^b	Yes (2)
23	23.01	447.0924	[C ₂₁ H ₁₉ O ₁₁] ⁻	-0.91	285 (C ₁₅ H ₉ O ₆)	328	Luteolin glycoside isomer	By MSMS	Yes (2)
24	23.22	467.2479	[C ₂₁ H ₃₉ O ₁₁] ⁻	-0.81	335 (C ₁₆ H ₃₁ O ₇), 233 (C ₉ H ₁₃ O ₇), 161 (C ₆ H ₉ O ₅), 101 (C ₄ H ₅ O ₃), 89 (C ₃ H ₅ O ₃)	219	Terpene diglycoside (Putative)	-	-
25	23.32	551.1416	[C ₂₁ H ₂₇ O ₁₄] ⁻	1.94	161 (C ₉ H ₅ O ₃)	219	cinnamoyl hydroxyloganin (PUTATIVE)	Putative;	
		701.2344	[C ₂₁ H ₃₉ O ₁₁] ⁻	5.70	539, 371 (C ₁₆ H ₁₉ O ₁₀), 307 (C ₁₅ H ₁₅ O ₇), 275 (C ₁₅ H ₁₅ O ₅), 223	220, 328	Oleuropein-glucoside or Aleuricine A/B		

					(C ₁₁ H ₁₁ O ₅), 179 (C ₆ H ₁₁ O ₆), 149 (C ₈ H ₅ O ₃)				
26	23.43	381.1555	[C ₁₉ H ₂₅ O ₈] ⁻	1.11	231 (C ₁₀ H ₁₅ O ₆), 201 (C ₉ H ₁₃ O ₅), 183 (C ₉ H ₁₁ O ₄), 151 (C ₉ H ₁₁ O ₂), 139 (C ₈ H ₁₁ O ₂)		HT-ACDE. (Hydroxytyrosylacyldihydro- -elenolate)	RT, MS, MSMS.	Yes (5)
27	23.54	573.2135	n.d.		345 (C ₁₅ H ₂₁ O ₉), 225 (C ₁₂ H ₁₇ O ₄), 209 (C ₁₀ H ₉ O ₅), 183 (C ₉ H ₁₁ O ₄), 165 (C ₉ H ₉ O ₃), 141 (C ₇ H ₉ O ₃), 121 (C ₈ H ₉ O)	219	Unknown	-	-
28	24.00	539.1771	[C ₂₅ H ₃₁ O ₁₃] ⁻	1.21	403 (C ₁₃ H ₂₃ O ₁₄), 223 (C ₁₁ H ₁₁ O ₅), 179 (C ₆ H ₁₁ O ₆), 119 (C ₄ H ₇ O ₄), 113 (C ₅ H ₅ O ₃), 101 (C ₄ H ₅ O ₃), 95 (C ₆ H ₇ O)	346	Oleuroside isomer	MS, MSMS	-
29	24.10	549.2870	n.d	2.32	417 (C ₂₁ H ₃₇ O ₈), 233(C ₉ H ₁₃ O ₇), 161 (C ₆ H ₉ O ₅).	219	Unknown		
		377.1241	[C ₁₉ H ₂₁ O ₈] ⁻	0.96	307 (C ₁₅ H ₁₅ O ₇), 275 (C ₁₄ H ₁₁ O ₆), 149 (C ₈ H ₅ O ₃), 139 (C ₇ H ₇ O ₃), 127 (C ₆ H ₇ O ₃), 111 (C ₅ H ₃ O ₃), 111 (C ₅ H ₃ O ₃), 101 (C ₄ H ₅ O ₃), 95 (C ₆ H ₇ O)		Oleuropein aglycone isomer	RT, MS, MSMS. And ref ^b	Yes (2)
30	24.29	569.1924	[C ₂₆ H ₃₃ O ₁₄] ⁻	-4.11	537 (C ₂₅ H ₂₉ O ₁₃) 403 (C ₁₇ H ₂₃ O ₁₁), 371 (C ₁₆ H ₁₉ O ₁₀), 305 (C ₁₅ H ₁₃ O ₇), 223 (C ₁₁ H ₁₁ O ₅), 151 (C ₈ H ₇ O ₃)		Methoxyoleuropein	RT, MS, MSMS. And ref ^b	Yes (2)
		527.2092	[C ₂₅ H ₃₅ O ₁₂] ⁻	4.72	377 (C ₁₆ H ₂₅ O ₁₀), 313 (C ₁₅ H ₂₁ O ₇), 101(C ₄ H ₅ O ₃)		Coumaroyl bearing derivative	MSMS	

		377.1241			307 (C ₁₅ H ₁₅ O ₇), 275 (C ₁₄ H ₁₁ O ₆), 197 (C ₁₀ H ₁₃ O ₄), 165 (C ₉ H ₉ O ₃), 149 (C ₈ H ₅ O ₃), 139 (C ₇ H ₇ O ₃), 121 (C ₈ H ₉ O), 111 (C ₅ H ₃ O ₃), 111 (C ₅ H ₃ O ₃), 101 (C ₄ H ₅ O ₃), 95 (C ₆ H ₇ O)		Oleuropein aglycone isomer	RT, MS, MSMS. And ref ^b	Yes (2)
31	24.61	539.1745	[C ₂₅ H ₃₁ O ₁₃] ⁻	-1.44	403 (C ₁₃ H ₂₃ O ₁₄), 371 (C ₁₆ H ₁₉ O ₁₀), 307 (C ₈ H ₁₉ O ₁₂), 275 (C ₁₅ H ₁₅ O ₅), 223 (C ₁₁ H ₁₁ O ₅), 179 (C ₆ H ₁₁ O ₆), 149 (C ₈ H ₅ O ₃), 119 (C ₄ H ₇ O ₄), 101 (C ₄ H ₅ O ₃), 95 (C ₆ H ₇ O)	222, 282	Oleuropein	RT, MS, MSMS. And ref ^b	Yes (2)
32	24.90	535.1430	[C ₂₅ H ₂₇ O ₁₃] ⁻	-1.61	389 (C ₁₆ H ₂₁ O ₁₁), 345 (C ₁₅ H ₂₁ O ₉), 307 (C ₁₅ H ₁₅ O ₇), 265 (C ₁₃ H ₁₃ O ₆), 235 (C ₁₂ H ₁₁ O ₅), 205 (C ₁₁ H ₉ O ₄), 163 (C ₉ H ₇ O ₃), 145 (C ₉ H ₅ O ₂), 121 (C ₈ H ₉ O)	219, 312	6'-(E)-p-coumaroyl-secologanoside	MS, MSMS	Yes (4)
33	25.16	539.1730	[C ₂₅ H ₃₁ O ₁₃] ⁻	1.91	403 (C ₁₃ H ₂₃ O ₁₄), 327 (C ₁₈ H ₁₅ O ₆), 307 (C ₁₅ H ₁₅ O ₇), 275 (C ₁₅ H ₁₅ O ₅), 223 (C ₁₁ H ₁₁ O ₅), 197 (C ₁₀ H ₁₃ O ₄), 165 (C ₉ H ₉ O ₃), 149 (C ₈ H ₅ O ₃), 139 (C ₇ H ₇ O ₃), 119 (C ₄ H ₇ O ₄), 101 (C ₄ H ₅ O ₃), 95 (C ₆ H ₇ O)	219	Oleuropein Isomer	RT, MS, MSMS. And ref ^b	Yes (2)
34	25.35	565.1511	[C ₂₆ H ₂₉ O ₁₄] ⁻	-4.04	345 (C ₁₅ H ₂₁ O ₉), 295 (C ₁₄ H ₁₅ O ₇), 235	220, 327	Unknown	-	-

					(C ₁₂ H ₁₁ O ₅), 193 (C ₁₀ H ₉ O ₄), 175 (C ₁₀ H ₇ O ₃), 161 (C ₉ H ₅ O ₃)				
35	25.62	539.1793	[C ₂₅ H ₃₁ O ₁₃] ⁻	3.35	403 (C ₁₃ H ₂₃ O ₁₄), 371 (C ₁₆ H ₁₉ O ₁₀), 327 (C ₁₈ H ₁₅ O ₆), 307 (C ₁₅ H ₁₅ O ₇), 275 (C ₁₅ H ₁₅ O ₅), 223 (C ₁₁ H ₁₁ O ₅), 197 (C ₁₀ H ₁₃ O ₄), 165 (C ₉ H ₀ O ₃), 149 (C ₈ H ₅ O ₃), 139 (C ₇ H ₇ O ₃), 119 (C ₄ H ₇ O ₄), 101 (C ₄ H ₅ O ₃), 95 (C ₆ H ₇ O)		Oleuroside Isomer	MS,MSMS	
36	25.77	543.2459	[C ₂₆ H ₃₉ O ₁₂] ⁻	2.31	375 (C ₁₆ H ₂₃ O ₁₀), 357 (C ₁₆ H ₂₁ O ₉), 227 (C ₁₂ H ₁₉ O ₄), 213 (C ₁₀ H ₁₃ O ₅), 199 (C ₁₁ H ₁₉ O ₃), 185 (C ₁₀ H ₁₇ O ₃), 169 (C ₉ H ₁₃ O ₃), 151 (C ₉ H ₁₁ O ₂), 125 (C ₇ H ₉ O ₂), 113 (C ₅ H ₅ O ₃)	220	Dihydro oleuropein	RT, MS, MS-MS	Yes (2)
37	25.99	535.1479	[C ₂₅ H ₂₇ O ₁₃] ⁻	3.33	389 (C ₁₆ H ₂₁ O ₁₁), 345 (C ₁₅ H ₂₁ O ₉), 307 (C ₁₅ H ₁₅ O ₇), 265 (C ₁₃ H ₁₃ O ₆), 235 (C ₁₂ H ₁₁ O ₅), 205 (C ₁₁ H ₉ O ₄), 163 (C ₉ H ₇ O ₃), 145 (C ₉ H ₅ O ₂), 121 (C ₈ H ₉ O)	220, 300	Coumaroyl-secologanoside isomer	MS. MS- MS	
38	26.30	377.1243	[C ₁₉ H ₂₁ O ₈] ⁻	0.29	307 (C ₁₅ H ₁₅ O ₇), 275 (C ₁₄ H ₁₁ O ₆), 171 (C ₇ H ₇ O ₅), 149 (C ₈ H ₅ O ₃), 139 (C ₇ H ₇ O ₃), 127 (C ₆ H ₇ O ₃), 113 (C ₅ H ₅ O ₃) 111	220, 286	Isomer of oleuropein aglycone	MSMS	

					(C ₅ H ₃ O ₃), 101 (C ₄ H ₅ O ₃), 95 (C ₆ H ₇ O)				
39	26.60	523.1780	[C ₂₅ H ₃₁ O ₁₂] ⁻	3.12	361 (C ₁₉ H ₂₁ O ₇), 291 (C ₁₅ H ₁₅ O ₆), 259 (C ₁₅ H ₁₅ O ₄), 101 (C ₄ H ₅ O ₃)	220, 276	Ligstroside (or isomer)	MSMS	Yes (6)
40	27.00	555.2100	[C ₂₆ H ₃₅ O ₁₃] ⁻	2.74	511 (C ₂₅ H ₃₅ O ₁₁) 345 (C ₁₅ H ₂₁ O ₉), 327 (C ₁₅ H ₁₉ O ₈), 225 (C ₁₂ H ₁₇ O ₄), 197 (C ₁₁ H ₁₇ O ₃), 183 (C ₁₀ H ₁₅ O ₃), 165 (C ₉ H ₉ O ₃), 155 (C ₅ H ₅ O ₃), 139 (C ₆ H ₃ O ₄), 121 (C ₈ H ₉ O)	220	Hydroxyoleurosides	RT, MS, MSMS and ref ^b	Yes (2)
41	27.15	493.1330	[C ₂₃ H ₂₅ O ₁₂] ⁻	-1.04	327 (C ₁₅ H ₁₉ O ₈), 209 (C ₁₀ H ₉ O ₅), 183 (C ₉ H ₁₁ O ₄), 165 (C ₉ H ₉ O ₃), 135 (C ₈ H ₇ O ₂), 121 (C ₇ H ₅ O ₂)	220	Unknown		
42	27.46	555.2040	[C ₂₆ H ₃₅ O ₁₃] ⁻	-3.20	345 (C ₁₅ H ₂₁ O ₉), 327 (C ₁₅ H ₁₉ O ₈), 225 (C ₁₂ H ₁₇ O ₄), 197 (C ₁₁ H ₁₇ O ₃), 183 (C ₁₀ H ₁₅ O ₃), 165 (C ₉ H ₉ O ₃), 155 (C ₅ H ₅ O ₃), 139 (C ₆ H ₃ O ₄), 121 (C ₈ H ₉ O)	220	Hydroxyoleurosides isomer	MS, MSMS	
43	27.70	377.1243	[C ₁₉ H ₂₁ O ₈] ⁻	0.21	307 (C ₁₅ H ₁₅ O ₇), 275 (C ₁₄ H ₁₁ O ₆), 191 (C ₁₀ H ₇ O ₄), 171 (C ₇ H ₇ O ₅), 149 (C ₈ H ₅ O ₃), 139 (C ₇ H ₇ O ₃), 127 (C ₆ H ₇ O ₃), 111 (C ₅ H ₃ O ₃), 101 (C ₄ H ₅ O ₃), 95 (C ₆ H ₇ O)	220	Isomer of oleuropein aglycone	RT, MS, MSMS and ref ^b	Yes (2)
44	28.10	461.2013	[C ₂₁ H ₃₃ O ₁₁] ⁻	-0.43	167 (C ₁₀ H ₁₅ O ₂)		Unknown	-	-

45	28.14	393.1191	[C ₁₉ H ₂₁ O ₉] ⁻	1.05	317 (C ₁₇ H ₁₇ O ₆), 181 (C ₉ H ₉ O ₄), 137 (C ₈ H ₉ O ₂)	220	Hydroxyoleuropein aglycone	Putative from MSMS data	-
46	28.29	557.2192	[C ₂₆ H ₃₇ O ₁₃] ⁻	-3.68	345 (C ₁₅ H ₂₁ O ₉), 227 (C ₁₂ H ₁₉ O ₄), 199 (C ₁₁ H ₁₉ O ₃), 185 (C ₁₀ H ₁₇ O ₃), 165 (C ₉ H ₉ O ₃), 139 (C ₆ H ₃ O ₄), 121 (C ₈ H ₉ O)	220,	6'-O-[(2E)-2,6-dimethyl-8-hydroxy-2-octenoyl]secologanoside	MSMS data	Yes (4)
47	29.95	545.2563	n.d.	-	-	-	Unknown	-	-
48	30.08	377.1242	[C ₁₉ H ₂₁ O ₈] ⁻	1.10	307 (C ₁₅ H ₁₅ O ₇), 275 (C ₁₄ H ₁₁ O ₆), 191 (C ₁₀ H ₇ O ₄), 171 (C ₇ H ₇ O ₅), 149 (C ₈ H ₅ O ₃), 139 (C ₇ H ₇ O ₃), 127 (C ₆ H ₇ O ₃), 111 (C ₅ H ₃ O ₃), 101 (C ₄ H ₅ O ₃), 95 (C ₆ H ₇ O)		Oleuropein aglycone	RT, MS, MSMS and ref ^b	Yes (2)
49	31.19	377.1243	[C ₁₉ H ₂₁ O ₈] ⁻	0.24	307 (C ₁₅ H ₁₅ O ₇), 275 (C ₁₄ H ₁₁ O ₆), 191 (C ₁₀ H ₇ O ₄), 171 (C ₇ H ₇ O ₅), 149 (C ₈ H ₅ O ₃), 139 (C ₇ H ₇ O ₃), 127 (C ₆ H ₇ O ₃), 111 (C ₅ H ₃ O ₃), 101 (C ₄ H ₅ O ₃), 95 (C ₆ H ₇ O)		Isomer of oleuropein aglycone	MSMS data	
50	32.21	943.3442	[C ₄₃ H ₅₉ O ₂₃] ⁻	0.05	513 (C ₃₅ H ₂₉ O ₄), 345 (C ₁₅ H ₂₁ O ₉), 227 (C ₁₂ H ₁₉ O ₄), 209 (C ₁₀ H ₉ O ₅), 185 (C ₁₀ H ₁₇ O ₃), 165 (C ₉ H ₉ O ₃), 149 (C ₈ H ₅ O ₃), 139 (C ₆ H ₃ O ₄), 121 (C ₈ H ₉ O), 101 (C ₄ H ₅ O ₃)	222	Unknown	-	-

Table. S3. Major compounds identified in fractions from the Koroneiki extract

Nr	Fraction	Major compounds
1	5	Hydroxytyrosol, Hydroxytyrosol glucoside, and Oleoside
2	6	Acyclodihydroelenolic acid glucoside isomer, Loganin
3	17	Rutin
4	18	Verbascoside
5	19	Dihydro oleuropein
6	20	Oleuropein glucoside
7	21	Oleuropein
8	22	Oleuropein and Coumaroyl-secloganoside
9	23	Dimethyl- Hydroxyoctenoyl-secologanoside
10	24	Hydroxyoleuropein aglycone, Oleuropein aglycone
11	25	Oleuropein aglycone
12	26	Oleuropein aglycone

References

1. Maalej, A., Bouallagui, Z., Hadrich, F., Isoda, H., and Sayadi, S. (2017) Assessment of *Olea europaea* L. fruit extracts: Phytochemical characterization and anticancer pathway investigation. *Biomedicine & Pharmacotherapy* **90**, 179–186
2. Michel, T., Khlif, I., Kanakis, P., Termentzi, A., Allouche, N., Halabalaki, M., and Skaltsounis, A.-L. (2015) UHPLC-DAD-FLD and UHPLC-HRMS/MS based metabolic profiling and characterization of different *Olea europaea* organs of Koroneiki and Chetoui varieties. *Phytochemistry Letters* **11**, 424–439
3. Rubio-Senent, F., Martos, S., Lama-Muñoz, A., Fernández-Bolaños, J. G., Rodríguez-Gutiérrez, G., and Fernández-Bolaños, J. (2015) Isolation and identification of minor secoiridoids and phenolic components from thermally treated olive oil by-products. *Food chemistry* **187**, 166–173
4. Obied, H. K., Prenzler, P. D., Ryan, D., Servili, M., Taticchi, A., Esposto, S., and Robards, K. (2008) Biosynthesis and biotransformations of phenol-conjugated oleosidic secoiridoids from *Olea europaea* L. *Natural product reports* **25**, 1167–1179
5. Obied, H. K., Karuso, P., Prenzler, P. D., and Robards, K. (2007) Novel secoiridoids with antioxidant activity from Australian olive mill waste. *Journal of agricultural and food chemistry* **55**, 2848–2853
6. Gariboldi, P., Jommi, G., and Verotta, L. (1986) Secoiridoids from *Olea europaea*. *Phytochemistry* **25**, 865–869